



저작자표시-비영리-변경금지 2.0 대한민국

이용자는 아래의 조건을 따르는 경우에 한하여 자유롭게

- 이 저작물을 복제, 배포, 전송, 전시, 공연 및 방송할 수 있습니다.

다음과 같은 조건을 따라야 합니다:



저작자표시. 귀하는 원저작자를 표시하여야 합니다.



비영리. 귀하는 이 저작물을 영리 목적으로 이용할 수 없습니다.



변경금지. 귀하는 이 저작물을 개작, 변형 또는 가공할 수 없습니다.

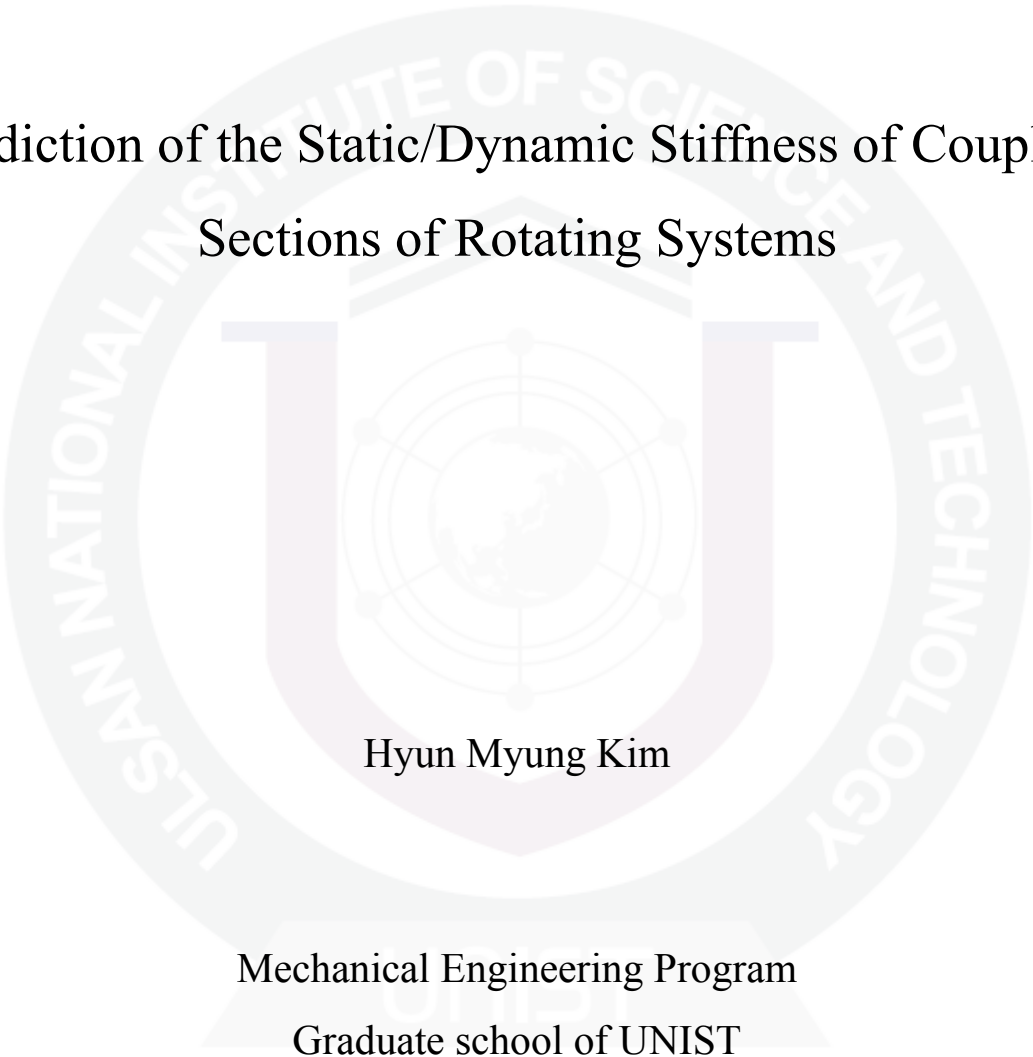
- 귀하는, 이 저작물의 재이용이나 배포의 경우, 이 저작물에 적용된 이용허락조건을 명확하게 나타내어야 합니다.
- 저작권자로부터 별도의 허가를 받으면 이러한 조건들은 적용되지 않습니다.

저작권법에 따른 이용자의 권리는 위의 내용에 의하여 영향을 받지 않습니다.

이것은 [이용허락규약\(Legal Code\)](#)을 이해하기 쉽게 요약한 것입니다.

[Disclaimer](#)

Prediction of the Static/Dynamic Stiffness of Coupling
Sections of Rotating Systems

The background features a large, light gray watermark of the UNIST logo. It consists of a circular emblem with the text "UNIST NATIONAL INSTITUTE OF SCIENCE AND TECHNOLOGY" around the perimeter. Inside the circle is a stylized 'U' shape containing a globe and a network of nodes and lines.

Hyun Myung Kim

Mechanical Engineering Program
Graduate school of UNIST

2012

Prediction of the Static/Dynamic Stiffness of Coupling Sections of Rotating Systems

Hyun Myung Kim

Mechanical Engineering Program
Graduate school of UNIST


Prediction of the Static/Dynamic Stiffness of Coupling Sections of Rotating Systems

A thesis
submitted to the Graduate School of UNIST
in partial fulfillment of the
requirements for the degree of
Master of Science

Hyun Myung Kim

07. 25 .2012

Approved by

A handwritten signature in black ink, appearing to read 'Park Wook', is written over a horizontal line.

Major Advisor

Hyung Wook Park

Prediction of the Static/Dynamic Stiffness of Coupling Sections of Rotating Systems

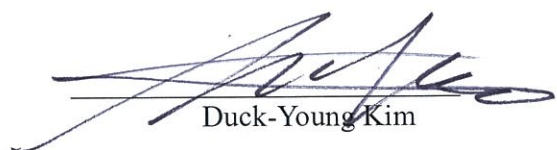
Hyun Myung Kim

This certifies that the thesis of Hyun Myung Kim is approved.

07.25.2012


Thesis Supervisor: Hyung Wook Park


Young-Bin Park


Duck-Young Kim

Abstract

Prediction of the Static/Dynamic Stiffness of Coupling Sections of Rotating Systems

Hyun Myung Kim

The School of Mechanical and Advanced Materials Engineering
The Graduate School
Ulsan National Institute of Science and Technology

The coupling section of rotating systems is a very important factor to determine their static/dynamic stiffness. To ensure the proper performance of the machine tool, the static/dynamic stiffness of the rotating system has to be predicted. Various parameters of the coupling section in rotating systems, such as the spring element, the node number and preload influence the characteristic of rotating system. This study focuses on the prediction of the static and dynamic stiffness of the rotating system with coupling section using the finite element (FE) model. To represent the coupling section of the rotating system, finite element method (FEM) computations on preload effect and the spring element arrangement were performed carried out. MATRIX 27 in ANSYS is the proper spring element to describe the coupling section of the rotating system because the MATRIX 27 can describe the coupling section close to the real object and is applicable to various rotating systems. The preload effect on the coupling section was estimated on the basis of the HERTZIAN contact theory. On the other hand, technical data for the specific ball bearings were obtained from bearing manufacturers. The FE model of the couple section which has the sixteen node using MATRIX 27 was constructed. Comparisons between FEM predictions and experimental results were performed in terms of the static and dynamic stiffness.

Contents

I . Introduction-----	1
1.1 Motivation-----	1
1.2 Research outline-----	3
1.3 Research objective-----	3
II . Literature review-----	4
2.1 Analytical method for prediction of static/dynamic stiffness-----	4
2.2 Experimental method-----	4
2.3 Finite element method-----	6
III . Coupling section modeling of rotating systems-----	9
3.1 General type of the coupling section-----	9
3.2 Coupling section modeling-----	10
3.2.1 Construction of the FE model-----	10
3.2.2 Selection of the connection type-----	13
3.2.3 Distribution method of the static stiffness within the coupling section-----	15
3.3 Hybrid coupling section-----	16
3.3.1 Overview of MATRIX 27-----	16
3.3.2 Applied MTRIX 27 in coupling section -----	18
3.3.3 Calibration matrix of model's rotating angle-----	19
3.4 Estimation of bearing stiffness under the preload-----	23
3.4.1 Preload effect in rolling bearing-----	23
3.4.2 Sensitivity analysis of the spring-----	23
3.4.3 Estimation of bearing stiffness under preload-----	24
IV . FEM prediction of the static /dynamic stiffness of the rotating system-----	27
V . Experimental verification-----	30

VI. FEA Automation-----	36
VII. Conclusions-----	38
VIII. Future works-----	39
References-----	40
Acknowledgment-----	42
Appendix-----	43

List of figures

- Figure 1.1 Overview of the general routine of the finite element simulation
- Figure 1.2 Research motivation
- Figure 1.3 Research scope
- Figure 2.1 Illustration of the experimental setup
- Figure 2.2 Overall view of the rotating system
- Figure 2.3 Research outline
- Figure 3.1 General type of the coupling system in the rotating
- Figure 3.2 Previous modeling of the coupling section in the rotating system
- Figure 3.3 Concept of simplified coupling section
- Figure 3.4 The number on coupling sections
- Figure 3.5 Flow chart of the coupling section modeling
- Figure 3.6 Stress distribution near the connecting node point
- Figure 3.7 The selected coupling section model
- Figure 3.8 Deformation of the spring element with the given load
- Figure 3.9 Advantage to built FE model for angular contact bearing
- Figure 3.10 Hybrid type of the connecting element using spring element.
- Figure 3.11 Limitation of COMBIN 14
- Figure 3.12 The rotational angle for coordinate transform
- Figure 3.13 The location of two reference point to estimate the rotational angle
- Figure 3.14 Verification of the calibrated FE model using MATRIX 27
- Figure 3.15 Sensitivity test
- Figure 3.16 Loading condition of rolling bearing.
- Figure 3.17 Estimation stiffness of bearing stiffness under the preload
- Figure 4.1 Overview of FEM prediction
- Figure 4.2 The constructed FE model
- Figure 4.3 Results of static and dynamic stiffness
- Figure 5.1 Illustration of the experimental setup
- Figure 5.2 Experimental configuration to implement the preload
- Figure 5.3 Experimental setup to test static stiffness
- Figure 5.4 Experimental setup to test dynamic stiffness
- Figure 5.5 Data acquisition system for the experiments

Figure 5.6 Comparison between FEM prediction and experimental results

Figure 5.7 The error of FEM predictions

Figure 6.1 Flow simulation based on internet

Figure 6.2 Procedure of FEA automation

Figure 6.3 Automation of MATRIX 27 for distribution matrix in FEM

List of tables

Table 1.Evaluation of the connecting type with changing node number

Table 2.The technical data of the angular contact ball bearing used in FEM simulation

I . Introduction

1.1 Motivation

A rotating system is being designed and manufactured with high performance in positioning accuracy and cutting stability. As a well recognized fact, the static and dynamic characteristic of a rotating system play an important role in determining the rotating system performance. Before fabrication of a prototype for performance identification, the designer should evaluate whether all the design requirements are satisfied in order to achieve the required performance in whole rotating system[1-3].

The simulation procedure has become important in the field of a rotating system. Since the many of the companies have wanted to reduce the time of development for production, time is related to cost. In the research filed, researchers have needed the characteristic of the rotating system easily and exactly for a variety of rotating units and systems. Thus, small businesses have also required the simulation method for developing their rotating system. However, they could not difficult to take the team of simulation on their own. In this trends, the commercial software of the simulation has accelerated to employ the prediction of the simulation for the characteristic in mechanical system though internet[4-6].

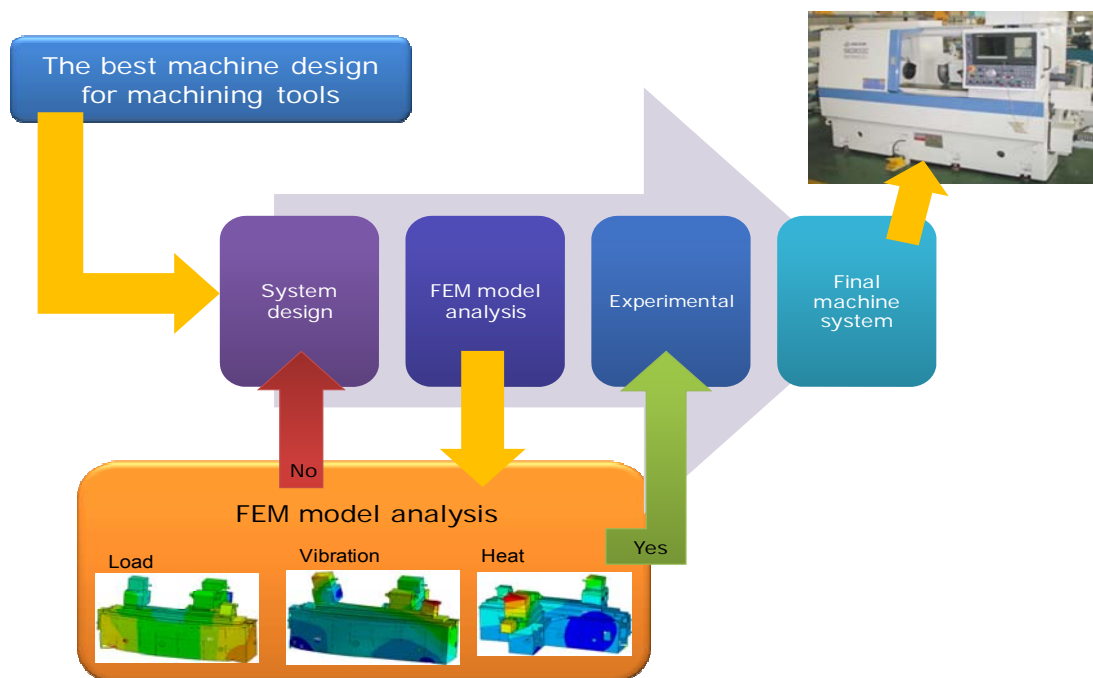


Figure 1.1 Overview of the general routine of the finite element simulation.

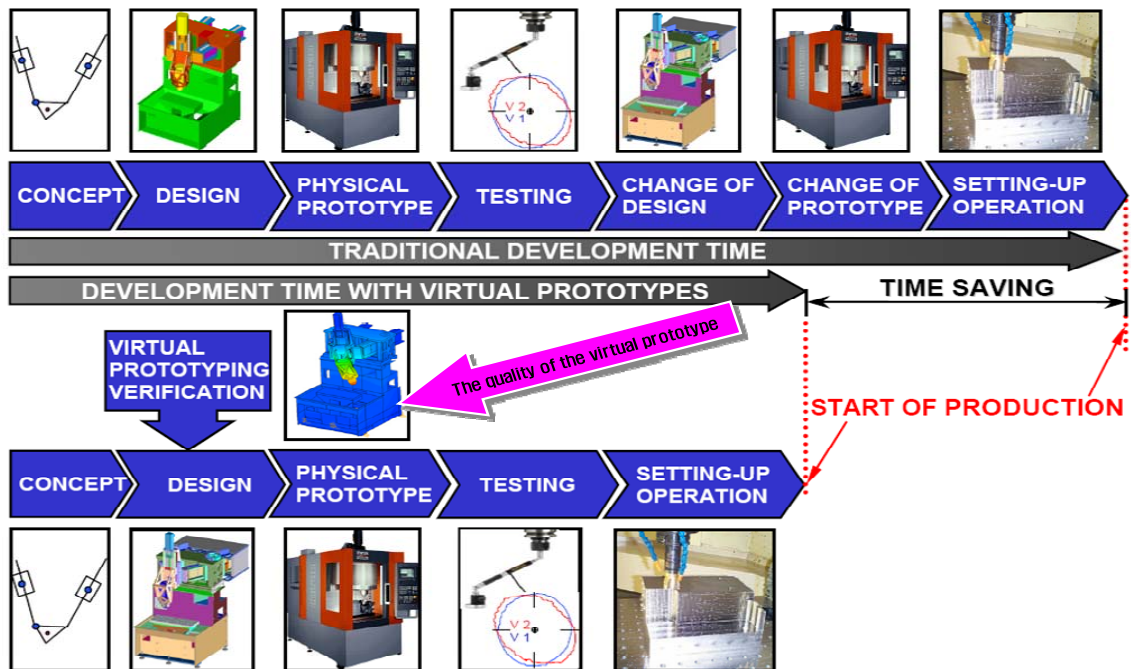


Figure 1.2 Research motivation.

Economic needs

- Spectrum of the structure as the model complexity and variety of new product development time/ cost explosion.
- Instead of actual prototype simulation analysis using a 3D virtual prototype-> the expensive experiment to remove -> Development time/ cost required shortening
- Structural/Thermal Analysis of the automation of small and medium enterprises need to relieve the shortage of skilled workers rotating system. However, they could not difficult to take the team of simulation on their own. In this trends, the commercial software of the simulation have accelerated to employ the prediction of the simulation for the characteristic in mechanical system though internet.

Engineering needs

- Underbelly of machinery and equipment identified in the design phase, this restructuring reflects the surge in demand.
- Interpreted as the automatic generation of boundary conditions for beginners, easy to use system requires analysis.
- Through a virtual prototype machine for extreme driving conditions simulated explosion behavior

1.2 Research outline

The rotating systems are designed with the modularity concept for satisfying the multipurpose or specific industrial applications. The rotating system was constructed with five main modules including the machine base, saddle, table, vertical column, and headstock with a spindle tool unit. The modules composed many joints. Its dynamic behavior is not only determined by these components but also by the dynamic characteristics of various joint. Researches of Zhang and Huang et al. show that about 60% of the total dynamic stiffness and about 90% of the total damping in a whole rotating system originates in the joints[7-9]. The rotating coupling section is important factor to predict the static and dynamic stiffness for rotating unit and system.

1.3 Research Objective

Above the research, FEM method was a useful model to predict the characteristic of rotating system. However, FEM has difficulty conducted the prediction of the rotating unit and system based on the original shape of coupling section because of the contact problems. Researchers have taken the simplified concept from the analytical method in order to apply to the coupling section of rotating unit such as bearing parts. The spring element in FE model has become key factor. Firstly, the coupling section of rotating unit has been defined using an spring element. This study has conducted the FEM prediction of rotating unit and system and then experimental verifications have been carried out.

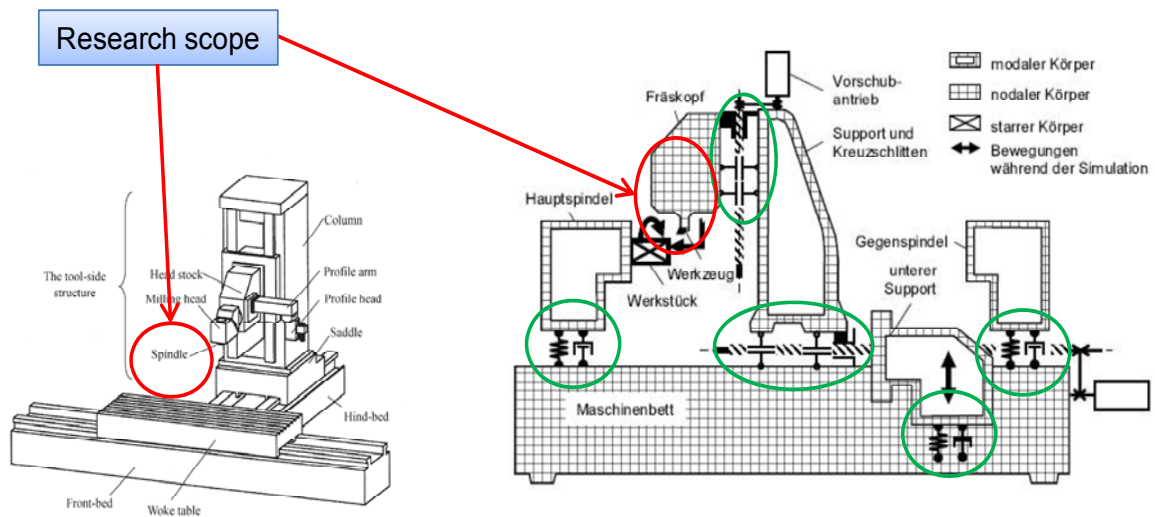


Figure 1.3 Research scope

II. Literature review

2.1 Analytical method for prediction of static/dynamic stiffness

Yang SHUN[10] has built a definition of static stiffness. He has studied the part of a spindle-nose using Maxwell's Reciprocal Theorem. John s Aqapou et al.[9, 11] have employed the rigid body deflection of a tool structure to predict a spindle tool holder tool system. Mathematical model was proposed to represent the defection of the tool clamped in the spindle because the spindle tool holder and tool holder tool interface linear and rotational stiffness should be estimated.

Erurk et al.[12] have predicted the spindle tool dynamic of tools based on Timoshenko beam model. He presented here, not only the tool, but all component of spindle-holder-tool assembly are modeled analytically and coupled in order to obtain tool point FRF by using receptance coupling and structural modification method. However, as neglect the effects of shear deformation and rotary inertia, Timoshenko beam theory is use for modeling their dynamics.

The most of the analytical way was studied in tool-holder[13]. It meant that the analytical model for rotating unit was difficult for static and dynamic stiffness. Thus, the many of the assumptions have been used in order to make 1-D solution[14-16] so the analytical approach could not apply for the various rotating unit and could not make the analytical model of whole structure model. Nevertheless, the concept of simplified model was very useful for real structure.

2.2 Experiment approach

A modal parameter identification of machine tool structures is conventionally achieved by obtaining frequency response curves from experimental data and then implementing a graphical approximation or fitting procedure. The principal shortcomings of this procedure originate from the inherent limitations of the Fourier Transform Method, used in obtaining the frequency responses, and from the subjective judgments of the analyst attempting to obtain the modal parameters by curve fitting. As an alternative to the conventional method, a direct modal parameter identification method, based on the dynamic data system approach, has been proposed. It utilizes data in the form of time series to develop discrete difference equations representing the dynamic properties of the machine tool structure at the points of measurement. The subsequent use of the models allows the determination of the global dynamic properties of the system such as the modal natural frequencies and damping ratios[16].

Zapciu et al[17]. have carried out a dynamic characterization and vibration analysis has been used for the detection and identification of machine tool condition for the natural frequencies of the lathe machining system. In the workspace model of machining, experimental procedure is implemented to determine the elastic behavior of the machining system such as constant operating speed, variable speed into a limited operating domain and imposed speed inside the operational domain[18, 19].

YAMAZAKI et al[20, 21]. have conducted the experiment of static stiffness for the rotating spindle. They have used the magnetic loading device and the grooved tool. It was possible to load to the spindle and Measure the static stiffness with the rotation speed. Shamine et al[22]. have present in-situ identification results for rolling element bearing parameter involved in machine tools by using frequency response function. They have conducted the study for different configuration of the spindle cutter system on a high speed milling machine[23-25].

The experiment could found the characteristic for whole system. However, the exact characteristic of rotating system needed a lot of experiment and each experiment cases have spent lot of money. It was serious problem to investigate the various rotating unit and system.

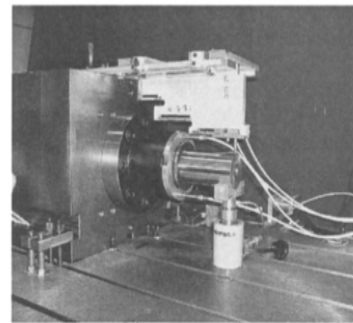
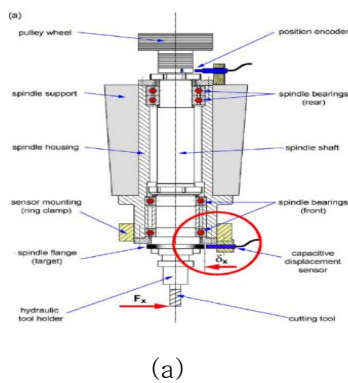


Figure 2.1 Illustration of the experimental setup : (a) sensor position of static stiffness (b) static stiffness (c) dynamic stiffness

2.3 Finite Element Method

Yuzhong Cao et al.[5]. developed a FE model for linear components with the implementation of contact stiffness at the rolling interface. To assess the dynamic characteristic and machining stability of a vertical milling system under the influence of a linear guide, researcher presented an approach of creating the spindle and machine frame coupled model, which provides the possibility of joining the spindle detailed dynamic model with the machine tool FE model.

Researches of Zhang and Huang et al.[7] show that about 60% of the total dynamic stiffness and about 90% of the total damping in a whole rating structure originates in the joints. A rotating system is a complicated system composed of many components with many joints. Its dynamic behavior is not only determined by these components but also by the dynamic characteristics of various joints.[8, 26] J.G.BoLLINGER et al.[13] presented a method of analysis for prediction of the static and dynamic behavior of machine tool spindle system. A mathematical model is formulated by use of the finite difference technique, and a general purpose analog computer is utilized to solve the equations in the model. A specific application is illustrated through the study of an actual lathe spindle. In analyzing the spindle behavior, the influences of bearing stiffness, bearing position, damping and the presence of the work piece are discussed. To enable a reduction of cost and time to market, fast and accurate predictions are required of the dynamic characteristics of new productions in the earliest stage of design. A growing number of these new products have rotating components, which are supported by rolling element bearings. Although ball and roller bearings have a significant and complex contribution to the dynamic behavior of machinery, they are often subjected to rigorous assumption in the case of modeling. At present many bearing models still fail to describe adequately the stiffness of the outer rings and the actual stiffness and mass distribution of the connecting bearing housings, the time-dependent variations of the bearing stiffness the damping in the elastohydrodynamically lubricated contacts and the vibrations generated by form deviations. Therefore, J A Wensing et al.[18] presented new method, which accurately describes the time dependent stiffness and mass properties of a rolling bearing application in an efficient way. The method enables a full transient analysis to study the effect of time dependent system properties, form deviations and mounting errors. Also the damping in ball and roller bearing is assessed, by comparing the results of advanced numerical simulations with experimental data. Deping Liu et al.[27] presented a method to investigate the characteristics of a high speed motorized spindle system. The geometric quality of high precision parts is highly dependent on the dynamic performance of the entire machining system, which is determined by the interrelated dynamics of machine tool mechanical structure and cutting process. This performance is of great importance in advanced, high-precision manufacturing processes.

The state of the art in machine tool main spindle units is focus on motorized spindle units for high speed and high performance cutting. They taking the high-speed milling motorized spindle of CX8075 produced by Anyang Xinsheng Machine Tool co. Ltd. as an example, a finite element model of the high speed motorized spindle is derived and presented. The model takes into account bearing support contact interface, which is established by spring-damper element COMBIN 14. Furthermore, the static analysis, model analysis, harmonic response analysis and thermal analysis were done by means of ANSYS commercial software.

Recently, many of the researchers have carried out the coupling section because when the coupling sections have been considered the rotating system of characteristic could have been presented. Thus, the FEM could have predicted the whole rotating system considering the coupling section. However, lots of the papers have conducted the investigation of joint for liner guile and bolt.[28-31] The rotating unit was the one of important parts in rotating system.[32-34] It has still remained early stage for coupling section until now day. It was not only the developing the coupling section for rotating unit and system but also the prediction of static and dynamic stiffness.

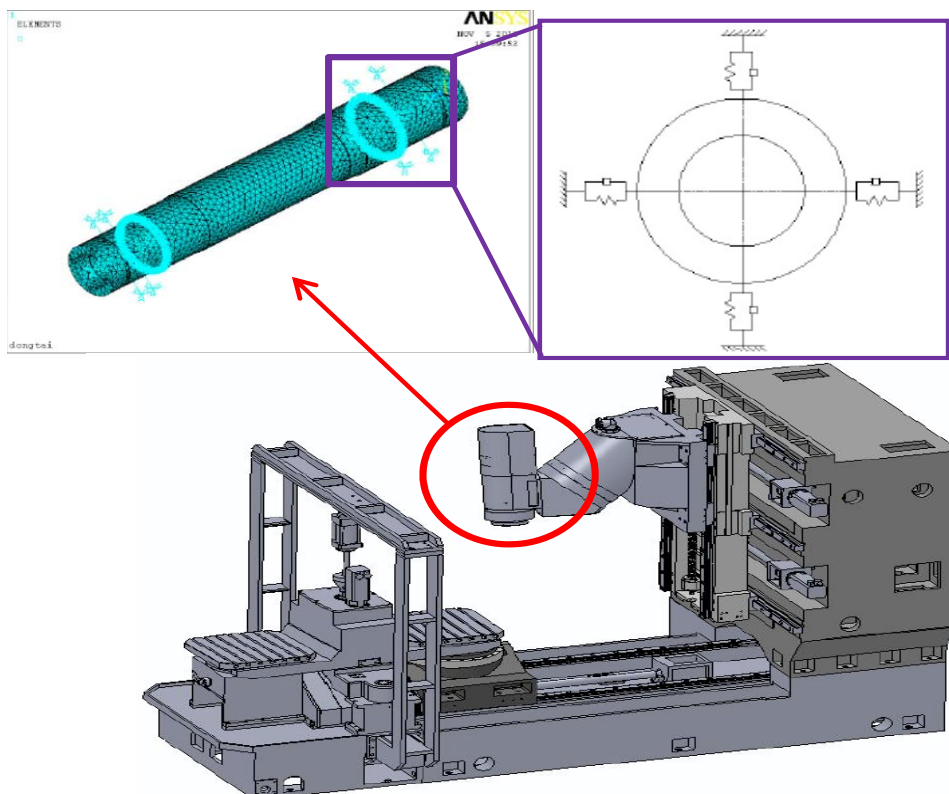


Figure 2.2 Overall view of the rotating system

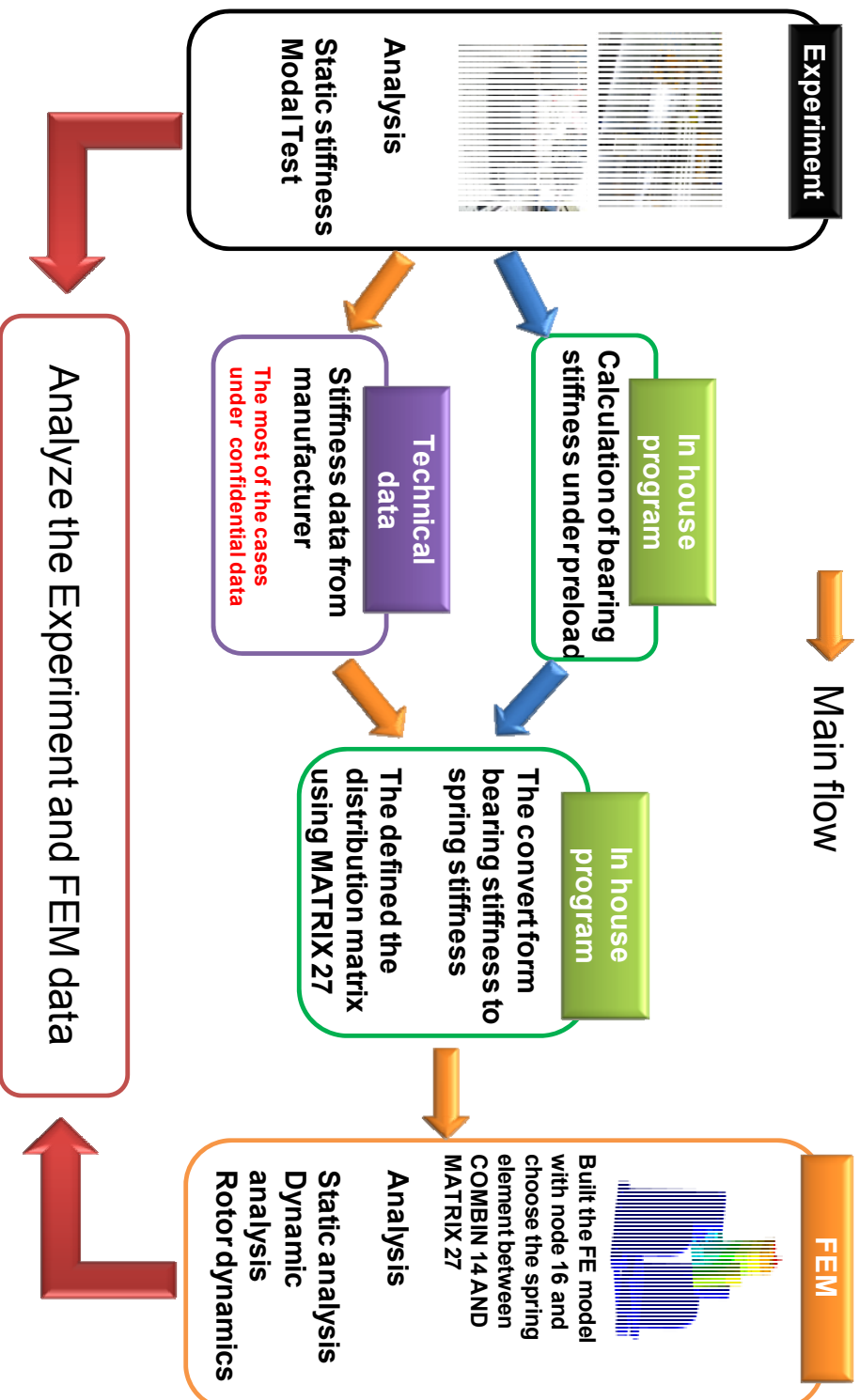


Fig 2.3 Research outline

III. Coupling section modeling of rotating systems

3.1 General type of the coupling section

A rolling bearing is that high precision spindle bearing combine good radial run-out and stiffness properties with low assembly and maintenance effort and a good cost effectiveness ratio. Despite their many advantages, the rolling bearings also have performance limitation, due to the geometry of the angular contact ball bearing. Radial displacement of the rolling bodies or radial widening of inner ring due to centrifugal forces or thermal expansion can lead to a relative axial displacement of the rings in the case of a bearing adjustment with constant preload.

Hydrostatic or hydrodynamic bearings are frequently used for high precision production task by given good damping and high stiffness. These have the advantage of achieving minimum radial and axial run out. As a result of increased heating of the fluid, due to internal shearing effect, there is a limit on the speeds with spindle having larger tool interfaces.

Aerostatic bearings are employed when much higher rotational speed need to be achieved. These work on the same principle as liquid-lubricated bearings, but the active medium is gaseous air with a lower viscosity than that of the liquids by two to three orders of magnitude. In order to realize a high load capacity and stiffness, very small clearance must be used within the bearings. Due to the low mass flow and small specific thermal capacity of air, the frictional heat produced by shear forces cannot be dissipated completely at high relative speed of the bearing components therefore require additional cooling.

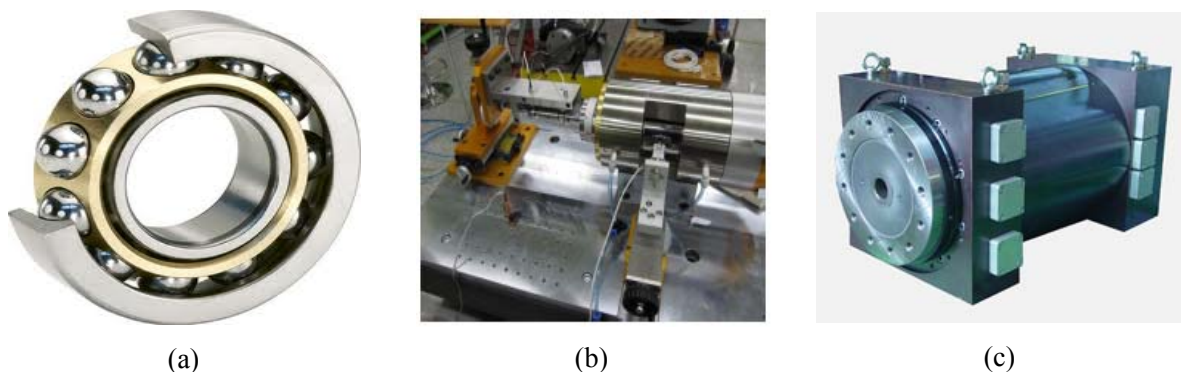


Figure 3.1 General type of the coupling system in the rotating system:(a) ball bearing (b) aerostatic bearing (c) hydrostatic bearing

3.2 Coupling section modeling

3.2.1 Construction of the FE model

The study makes the development of coupling section for FEM compared to early stage modeling method. For predicting a behavior on rotating units, researches proposed a lot of FE model. However, the models have been limited in order to present the simulation about a whole model. They have also restricted high guilty predictions to static and dynamic stiffness in full scale, because there were some problems.

Earlier researches took a FE model based on a real shape of a bearing. They have applied for a contact method to the model. It needed high computational power and technical ability to get the accurate prediction. Besides, the computational time was too long. Other researches proposed the spring element instead of the bearing on rotating units. It could make the ease and simple procedure but it only carried out rotating unit not to expend the system levels. Fig 3.2 was shown above matters.[31, 33, 35]

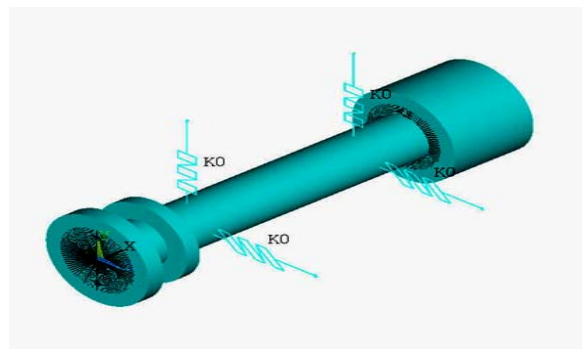
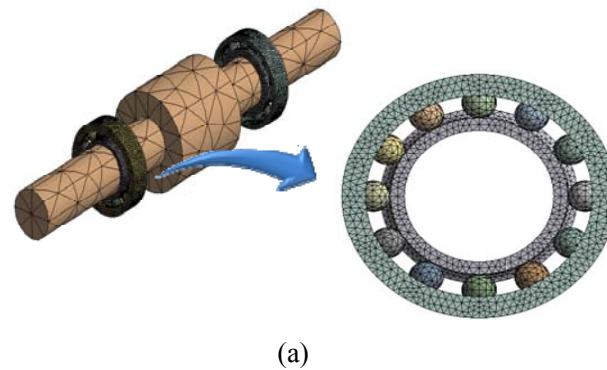


Figure 3.2 Previous modeling of the coupling section in the rotating system: (a) real shape modeling (b) Applied spring element modeling

The full scale of the simulation for the rotating system has needed the new concept of bearing joint, because the FE model reduced a gap of a real behavior. The study tried to change from balls to spring elements when the bearing has been created on 3D CAD model. The simple coupling section model has been taken (Fig 3.3).

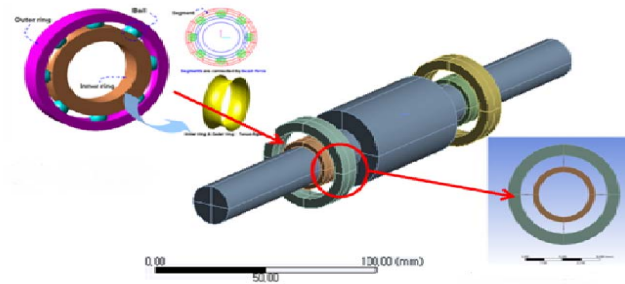
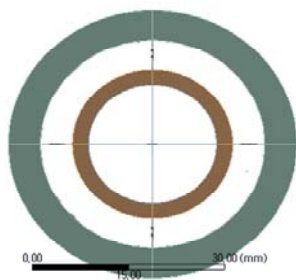
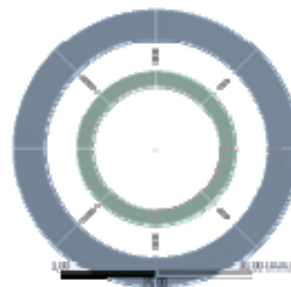


Figure 3.3 Concept of the simplified coupling section



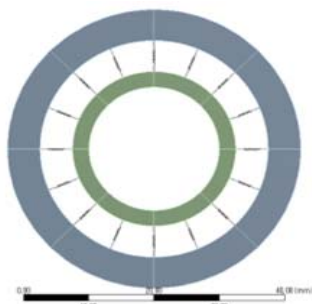
node: 4

(a)



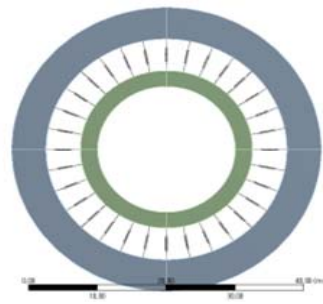
node: 8

(b)



node: 16

(c)



node: 32

(d)

Figure 3.4 The number on the coupling section:(a) 4 (b) 8 (c) 16 (d) 32

The simple model of the coupling section for rotating units consisted of inner race, outer race and a spring element. One of the key points was inner and outer race that the real bearing has. It could make the rotating unit attach the system levels structure. The bearing stiffness could have been defined in FE model for the prediction of static and dynamic stiffness.

Another key point was how many nodes the model has on inner and outer race. The coupling section for rotating units had the different distribution to bearing stiffness according to the number of nodes in there. The static and dynamic stiffness have also been related. Therefore, the several models have been suggested to make the specific bearing model for static and dynamic stiffness. Each model was seen in Fig 3.4. To take spring element's position between inner and outer race, connect points were necessary on the surface of inner and outer race. They have been conducted on modeling step using the function of surface partition. There is whole procedure for modeling in Fig 3.5.

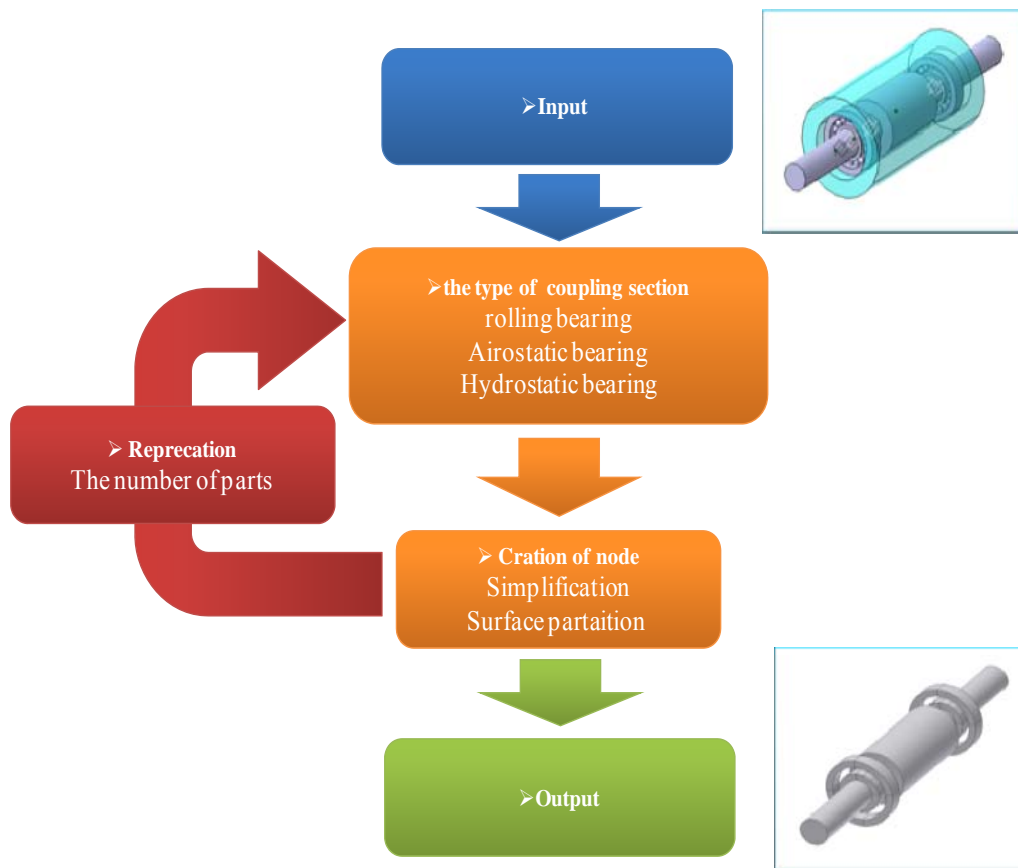


Figure 3.5 Flow chart of the coupling section modeling

3.2.2 Selection of the connection type

The final model has been chosen under several evaluation factors that are a stress distribution, application spring element, Identity between FE model and bearing and level of difficulty about model. This study has proposed the five models under the different node. Firstly, the stress distribution has been considered within inner race and outrace. Previous study has only used the four node of model in FE model. However, the model could not express the stress distribution in inner race and outer race. It has led stress concentration in a connection point. It does not make sense to observe the stress distribution in real case. To inform difference for the stress distribution between models, the static analysis has been conducted. The value of the stress has taken the sampling section that is nearby the connecting point. The different stress distribution has been presented according to the number of the node. When the number of nodes has increased in model, Stress concentration has been changed to stress distribution. However, the number of node 32 had the stress distortion in model. It does make sense on fourth point in sampling section because fourth point had to get higher stress than other points.

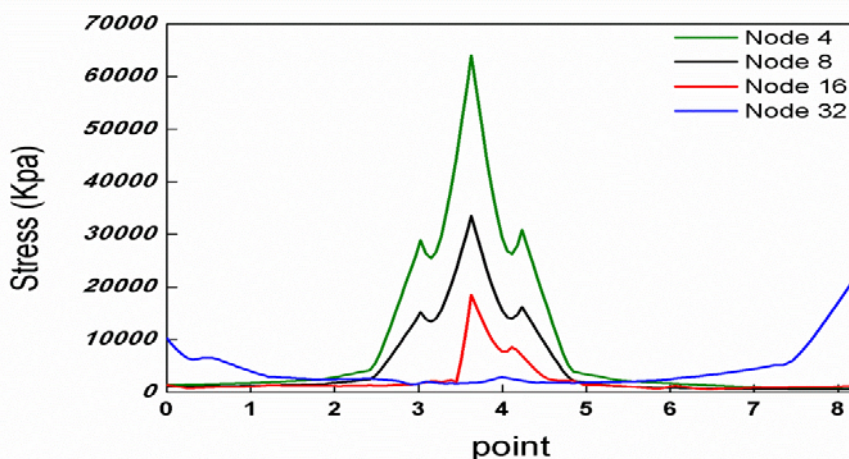
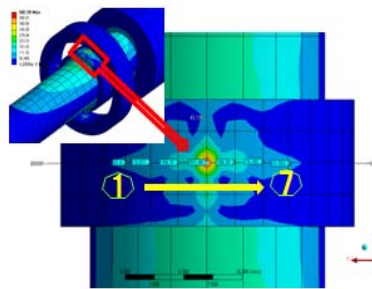
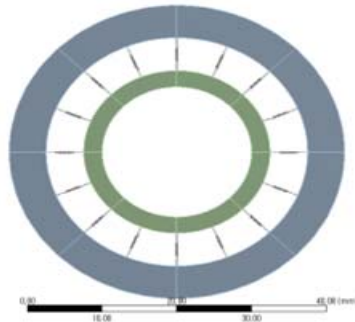


Figure 3.6 Stress distribution near the connecting node point

Secondly, the minimum of node have to be node 16 because of MATRIX 27. MATRIX 27 could not consider the stiffness and damping in one element. It should need the double node compared to COMBIN 14.

Finally, the minimum of number of balls in rolling bearing has been considered to define the arrangement in coupling section. For closing the real coupling section, the best way was that the number of node has same for number of balls in bearing. However, it was not ease to make model in modeling stage. So the coupling section had realty in coupling section. The minimum of number of twelve has been looked in from papers and technical data.

The number of node 16 was best model from evaluation of factors. The compared data was represented in table. 1.



Node : 16

Figure 3.7 The selected coupling section model

Table 1.Evaluation of the connecting type with changing node number

	Node 4	Node 8	Node 16	Node 32
Stress distribution	+	++	+++	+
Spring element application	-	++	++++	++++
Level of difficulty for model	++++	+++	++	+
Identity between FE model and bearing	+	++	+++	++++

3.2.3 Distribution method of the static stiffness within the coupling section

The model of coupling section has to situate the spring element between inner race and out race. It already explained the concept of the modeling step. It was just geometry. For simulation, Making the simple bearing model had to go next step that is how to defined the property of the spring element stiffness form bearing stiffness. Because the bearing stiffness meant the total stiffness of simple bearing model which consisted of the spring element set. It told us that bearing stiffness and spring stiffness were different idea in view of the fact that the bearing stiffness applied to spring element directly. In this regard, a mathematic form was required to distribute the bearing stiffness to the simple model. It has been proved in the model of 16 nodes so general form of equation has been driven. For the equation the energy method have been taken to the 16 nodes model.(Fig.3.9).

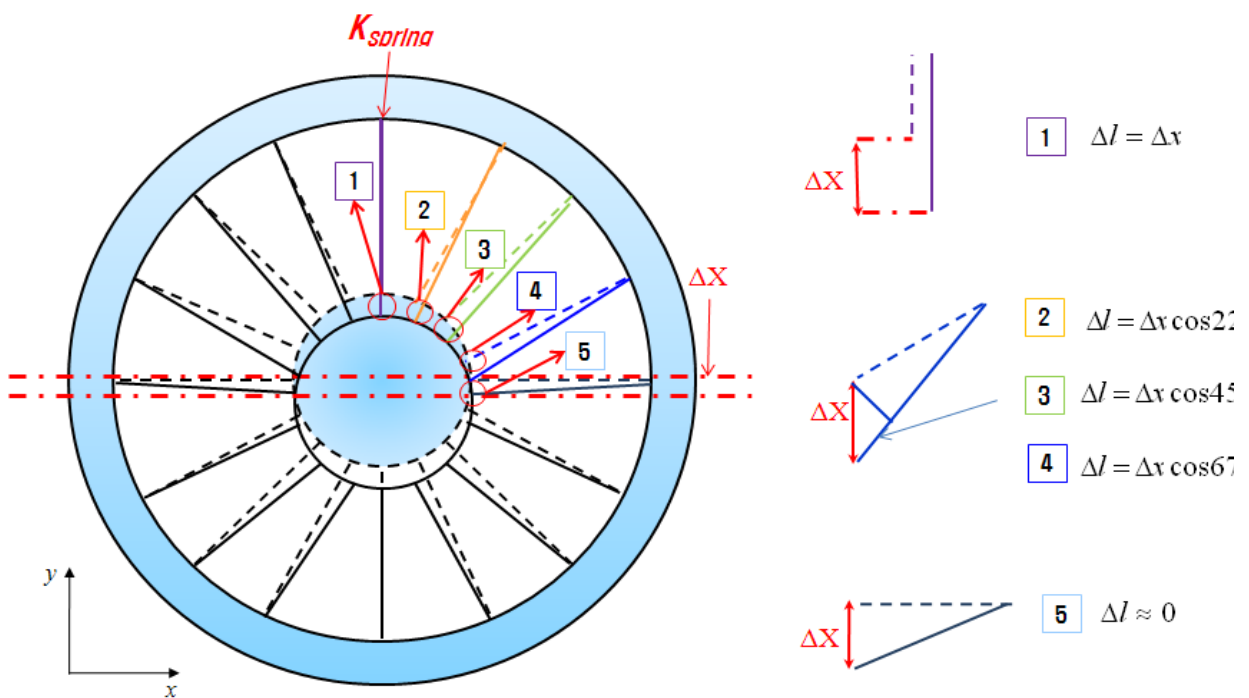


Figure 3.8 Deformation of the spring element with the given load

$$S_1 = \frac{1}{2} K_{spring} x^2 \quad (1)$$

$$S_2 = \frac{1}{2} K_{spring} (\cos 22.5 x)^2 \quad (2)$$

$$S_3 = \frac{1}{2} K_{spring} (\cos 45 x)^2 \quad (3)$$

$$S_4 = \frac{1}{2} K_{spring} (67.5 x)^2 \quad (4)$$

Above equations have only derived the upper part of the model. To cover the whole mode for the elastic deformation energy of the bearing stiffness, it was the double of the sum above the equations.

$$\frac{1}{2} K_{bearing} = 4 K_{spring} x^2 \quad (5)$$

$$K_{spring} = \frac{K_{bearing}}{8} \quad (6)$$

Above the equation based on nodes 16, it could infer the general equation of the specific model. The general equation was below.

$$K_{radial_spring} = \frac{K_{radial_bearing_stiffness}}{(0.5 \times N_{number_of_node})} \quad (7)$$

It could convert from bearing stiffness to spring stiffness on the simple bearing model.

3.3 Hybrid coupling section

3.3.1 Overview of MATRIX 27

Four of the spring elements for a coupling section have existed in ANSYS such as Combination 24, Matrix 27, Combination 214 and Combination 40. The element choice depends on shape, cross terms and

Nonlinearities. Spring is an elastic element that is used to store mechanical energy and which retains its original shape after a force is removed. Springs are typically defined in a stress free or unloaded state. This means that no longitudinal loading conditions exist unless preloading is specified

The study has investigated MATRIX 27 because of the important factor to develop the coupling section. MATRIX27 represents an arbitrary element whose geometry is undefined but whose elastic kinematic response can be specified by stiffness, damping, or mass coefficients in matrix form. The matrix is assumed to relate two nodes, each with six degrees of freedom per node: translations in the nodal x, y, and z directions and rotations about the nodal x, y, and z axes. See MATRIX27 in the Theory Reference for the Mechanical APDL and Mechanical Applications for more details about this element. The element is defined by two nodes and the matrix coefficients. The stiffness, damping, or mass matrix constants are input as real constants. All matrices generated by this element are 78 by 78. The degrees of freedom are ordered as UX, UY, UZ, ROTX, ROTY, ROTZ for node I followed by the same for node J. If one node is not used, simply let all rows and columns relating to that node default to zero. A structural matrix that combines the effects of many elements is normally positive or zero definite, as are the element matrices that contribute to it. There may be unusual circumstances where an element matrix is negative definite, and this is okay if there are other matrices connected to the same nodes that are positive definite, resulting in a final system of equations is still positive or zero definite. A simple example of such a circumstance is a beam element loaded with half of the buckling load. The stress stiffness matrix is negative definite, but the combined regular and stress stiffness matrix is positive definite.

In case of FE model, The modeling procedure could be reduced when the MATRIX 27 has been used for angular contact ball bearing. It could decrease the number of nodes and computation power.

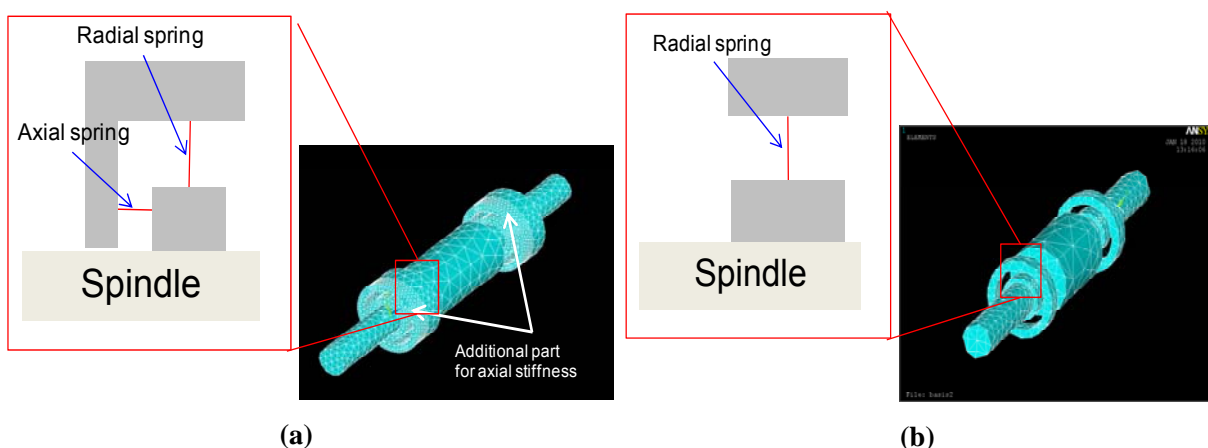


Figure 3.9 Advantage to built FE model for angular contact bearing : (a) FE model based on COMBIN 14 (b) FE model based on MATRIX 27

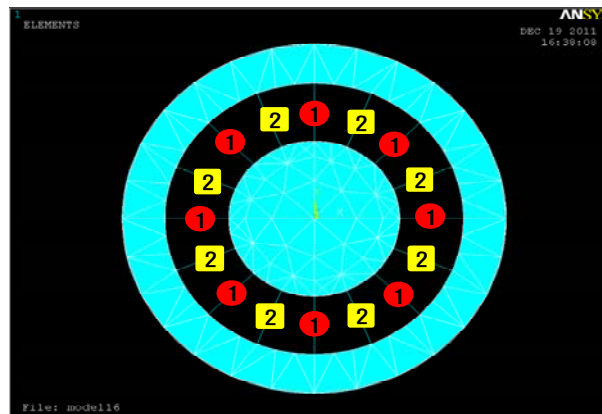
3.3.2 Applied MATRIX 27 in coupling section

The MATRIX 27 has several benefits compared to Combination 14. To begin with, the spring stiffness could define X, Y and Z in global coordination. It was a powerful function so as to build the angular contact bearing in FEM. However, MATRIX 27 did not unite into element for the function of stiffness and damping. For using the MATRIX 27, there was the equation on stiffness and Damping coefficient below. In case of the spring stiffness, the initial spring stiffness matrix has been made. Therefore, the axial and radial spring stiffness has been converted from axial and radial bearing stiffness. So the general equation has been modified for MATRIX 27.

$$K_{radial_spring} = \frac{K_{radial_bearing_stiffness}}{(0.5 \times N_{number_of_node})} \quad (8)$$

$$K_{axial_spring} = \frac{K_{axial_bearing_stiffness}}{(N_{number_of_node})} \quad (9)$$

$$K_{initial} = \begin{pmatrix} K_{radial_spring} & & \\ & & \\ & & K_{axial_spring} \end{pmatrix} \quad (10)$$



Stiffness (K) : 1

Damping(C) : 2

Figure 3.10 Hybrid type of the connecting element using spring element

According to the position of the spring at radial direction, the stiffness matrix has considered the position effect as the bearing stiffness has uniformly been distributed in the simple bearing model.

$$K_{DSM}(\theta) = \begin{pmatrix} \cos \theta & \sin \theta & 0 \\ -\sin \theta & \cos \theta & 0 \\ 0 & 0 & 1 \end{pmatrix} \begin{pmatrix} & & \\ & K_{\text{initial}} & \\ & & \end{pmatrix} \begin{pmatrix} \cos \theta & \sin \theta & 0 \\ -\sin \theta & \cos \theta & 0 \\ 0 & 0 & 1 \end{pmatrix}^T \quad (11)$$

Damping coefficient has followed the same procedure above.

$$D_{DDM}(\theta) = \begin{pmatrix} \cos \theta & \sin \theta & 0 \\ -\sin \theta & \cos \theta & 0 \\ 0 & 0 & 1 \end{pmatrix} \begin{pmatrix} & & \\ & D_{\text{initial}} & \\ & & \end{pmatrix} \begin{pmatrix} \cos \theta & \sin \theta & 0 \\ -\sin \theta & \cos \theta & 0 \\ 0 & 0 & 1 \end{pmatrix}^T \quad (12)$$

3.3.3 Calibration matrix of model's rotating angle

Researchers have usually chosen the Combination 14 which was the type of spring element in ANSYS. COMBIN14 has longitudinal or torsional capability in 1-D, 2-D, 3-D applications. The longitudinal spring-damper option is a uniaxial tension-compression element with up to three degrees of freedom at each node. No bending or torsion is considered. The tensional spring-damper option is a purely rotational element with three degrees of freedom at each node.

It could easily use the FE model and took the two functions about stiffness and damping coefficient. However, the spring element had a serious problem in specific model which have amount angle in Cartesian coordination system. The simple bearing model consisting of the combination 14 expressed the bearing stiffness in case of rotating the model in typical axis such as x, y and z. The problem has been proved by contacting the FEM of static analysis on the one case with Combination 14. The simple bearing model of nodes 16 has been created with 45 degree in Z axis. The bearing stiffness has been ensured about 1N/um. A force with 1N gave the model a radial direction. Fig.4 showed the deformation of a radial direction was not uniform. It means that the static

Stiffness of rotating unit should not have reliability in case of getting specific angle. The reason was that Combination 14 being twisted in 3 dimensions has made the bearing stiffness non-uniform in model. Besides, there was nothing for the method of compensation. Another weakness was that the additional part in the simple bearing model has been created to axial direction in order to assign the axial stiffness in case of the angular contact bearing. It should lead to increase the node and the procedure in FEM, now that it took time to conduct the subordinate processing.

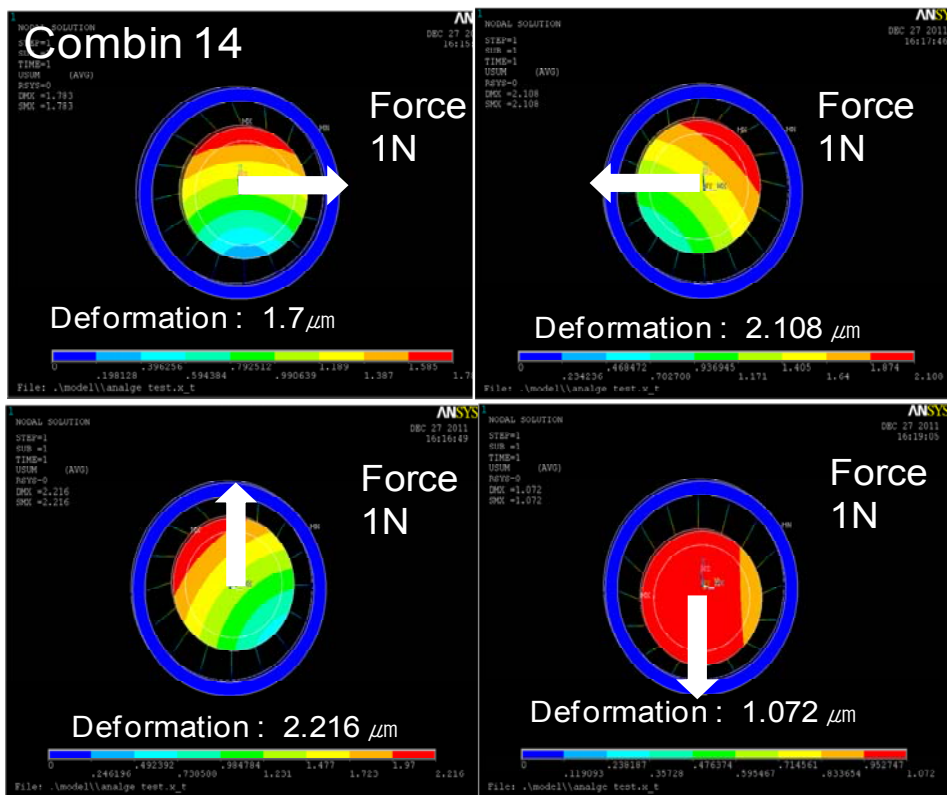
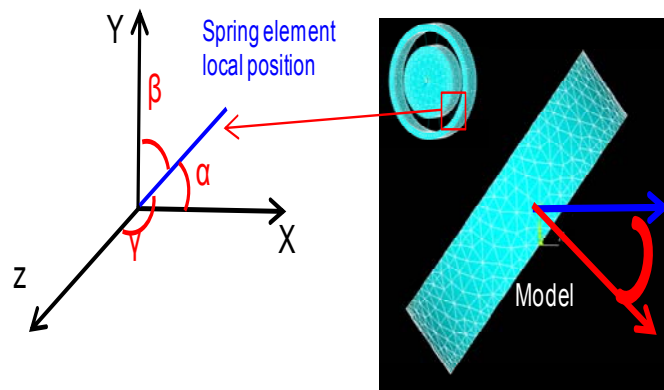


Figure 3.11 Limitation of COMBIN 14

However, MATRIX 27 could be calibrated for stiffness matrix when the axis of rotating unit didn't coincide the global axis such X, Y and Z. as considered the position effect as the bearing stiffness has uniformly been distributed in the simple bearing model. For calibration major angles have defined α , β , γ on X, Y and Z. However, γ could be ignored because the stiffness matrix of rotating unit could cover it up. The unit direction vector of rotating unit was important in order to calculate the turn angles in coordination. It has been obtained from punctual coordinates at center point in rotating unit.

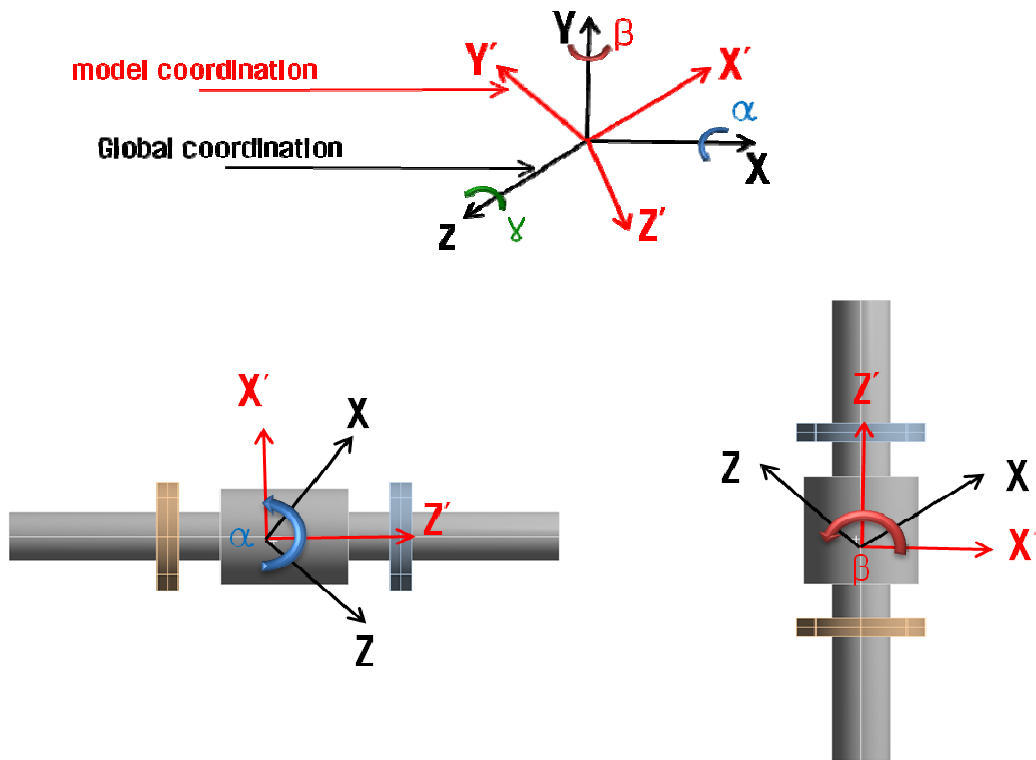


Figure 3.12 The rotational angle for coordinate transform

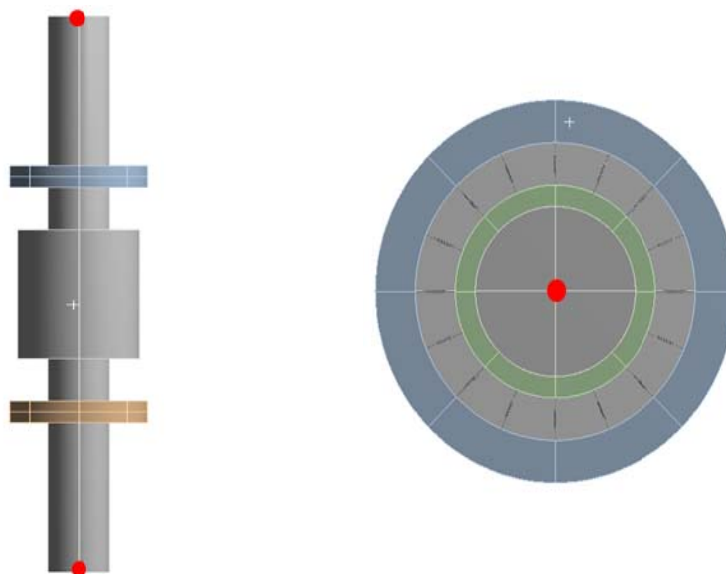


Figure 3.13 The location of two reference point to estimate the rotational angle

The turn angle has been calculated from the punctual coordinates.

$$\alpha = \sin^{-1} \left(\frac{y_1}{\sqrt{y_1^2 + z_1^2}} \right) \quad (13)$$

$$\beta = \cos^{-1} \left(\frac{z_1}{\sqrt{x_1^2 + z_1^2}} \right) \quad (14)$$

The Matrix of coordinate transform for calibration was below.

$$M_{RTM}(\alpha, \beta, \gamma) = \begin{pmatrix} \cos(\beta)\cos(\gamma) & -\cos(\alpha)\sin(\gamma) + \sin(\alpha)\sin(\beta)\cos(\gamma) & \sin(\alpha)\sin(\gamma) + \cos(\alpha)\sin(\beta)\cos(\gamma) \\ \cos(\beta)\sin(\gamma) & \cos(\alpha)\cos(\gamma) + \sin(\alpha)\sin(\beta)\sin(\gamma) & -\sin(\alpha)\cos(\gamma) + \cos(\alpha)\sin(\beta)\sin(\gamma) \\ -\sin(\beta) & \sin(\alpha)\cos(\beta) & \cos(\alpha)\cos(\beta) \end{pmatrix} \quad (7)$$

For verification of MATRX 27 the FE model of the bearing model conducted under force of 1N, axial stiffness of 100N/μm, radial stiffness of 1 N/μm and the β of 45.r point in rotating unit. The result of the FEM showed the Fig. 9. The Error has been decreased within 10%. It should inform the calibration of the spring element on the coordination.

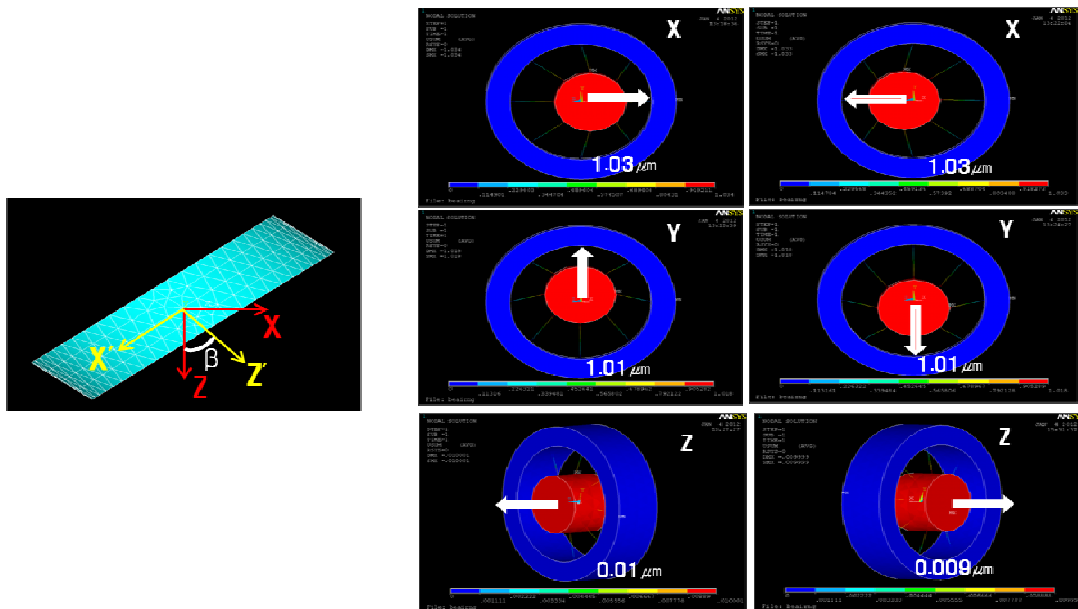


Figure 3.14 Verification of the calibrated FE model using MATRX 27

3.4 Estimation of bearing stiffness under pre-load

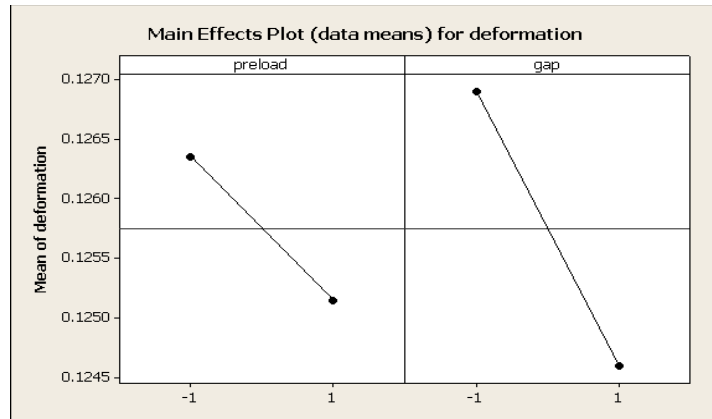
3.4.1 Pre-load effect in rolling bearing

Initial axial pre-load of rolling element bearing is commonly used to obtain high stiffness of rotating unit. It is known that the preload appears when an axial load is applied to a bearing at the assembly state. Generally, a higher pre-load would reduce the shaft deflection under the load, but might also decrease the bearing life. Therefore, pre-load should not be higher than necessary for the application but should be sufficient to avoid the pre-load being completely relieved from any bearing by action of external load. Therefore, a certain minimum preload is necessary to seat all of the balls and insure firm rolling contact. If this level of pre-load is not reached, balls will intermittently skid and roll and produce cage- ball instability. When this occurs, vibration levels may be one or even two orders of magnitude higher than that normally associated with bearing. In the end, the precise prediction of static and dynamic stiffness on rotating unit has to consider the preload effect. That is one of the important factors in coupling section.

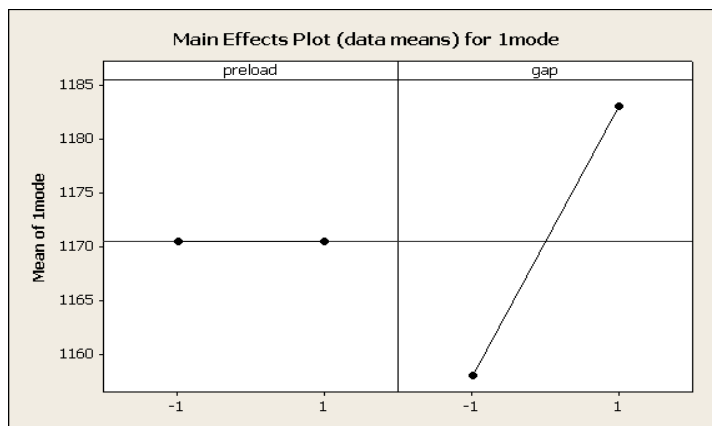
3.4.2 Sensitivity analysis of the spring

Early stage, the function of preload in COMBIN 14 has been focused to consider the pre-load effect in FEM. It could apply to model easily and could not additional procedure. To investigate the function of pre-load in spring element, sensitivity test have been conducted using commercial software about MINITAB. The sensitivity test has designed the two levels under the two factors. One was the size of gap between inner and outer race. That was original size of 10mm and half size. Another was pre-load. The conditions of pre-load were 0 N and 5000N. When the two levels of sensitivity test have been conducted, one of factors has defined much higher value than the others. When the number of node has increased in model, Stress concentration has been changed to stress distribution. However, the number of node 32 had the stress distortion in model. It does make sense on fourth point in sampling section because fourth point had to get higher stress than other points.

The result of the sensitivity test has represented that the size of gap is significantly influence in static and dynamics stiffness. The gap size has fixed the gap size of 10mm in order to avoid the additional geometry error in this study. However, the preload function in COMBIN 14 has not worked efficiently in FEM. The static stiffness had difference owing to preload. In case of dynamics stiffness, there was not any difference. It has told us that the preload function of COMBIN 14 is unsuitable.



(a)



(b)

Figure 3.15 Sensitivity test :(a) Deformation (b) Natural frequency

3.4.3 Estimation of bearing stiffness under pre-load

The influence of pre-load has classified the geometrical calibration and the characteristic of bearing stiffness.[36-38] The characteristic of bearings stiffness under pre-load was more important than the geometrical calibration on static and dynamic stiffness. Because the coupling section composed of the spring element that is dependable on bearing stiffness, pre-load effect has considered the relationship between preload and bearing stiffness. Although the geometrical calibration was also important factor in real cases, it could not represent the behavior of spindle in FEM. This study has focused on the characteristic of bearing stiffness under the preload. To calculate the bearing stiffness on preload, the equation had to be need for rotating unit. The first step was the force equilibrium about relationship of preload and the deflection force on the ball of bearing. And then the deflection of balls in rolling bearing

has been predicted using Hertz's contact theorem about point to point contact.

Assume that the contact forces on each ball of the ball bearing are equal when the rolling bearing is under load F. The loading conditions of the rolling bearings are shown in Fig. 20. The equilibrium condition of the rolling bearing is show in Eq.(26) and Eq.(27).

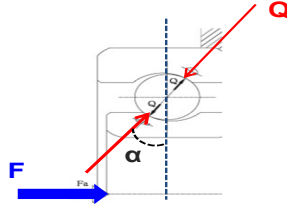


Figure 3.16 Loading condition of rolling bearing.

$$F_{axial} = n \cdot Q \cdot \sin(\alpha) \quad (15)$$

$$F_{radial} = n \cdot Q \cdot \cos(\alpha) \quad (16)$$

Where Q is the contact force of each ball, α is the contact angle, n is number of the ball.

For the rolling bearing, the contact stiffness of the interface between the inner race and outer race can be related to the local deformation at the point where rolling ball and raceway contact. By using the Hertz contact Theory, the deformation can be expressed blew.[39]

$$\delta_T = 2 \cdot m \sqrt{\frac{3 \cdot Q}{E_R \rho_h}} \quad (17)$$

Where Q denotes the contact force, m is coefficient which characterizes the pressure distribution between bodies, E_R is the reduced modulus of elasticity in tension and ρ_H is the sum of the surface curvature radiuses. They can be obtained from Eqs. (26),(27) and (28) combined.

$$\delta_{axial} = \frac{\delta_T}{\sin(\alpha)} \quad (18)$$

$$\delta_{radial} = \frac{\delta_T}{\cos(\alpha)} \quad (19)$$

Thus, the axial and radial stiffness is

$$K_{axial} = \frac{F_{axial}}{\delta_{axial}} \quad (20)$$

$$K_{radial} = \frac{F_{radial}}{\delta_{radial}} \quad (21)$$

The bearing stiffness has followed the trend of bearing stiffness compared with technical data. However, estimation of bearing stiffness has errors.

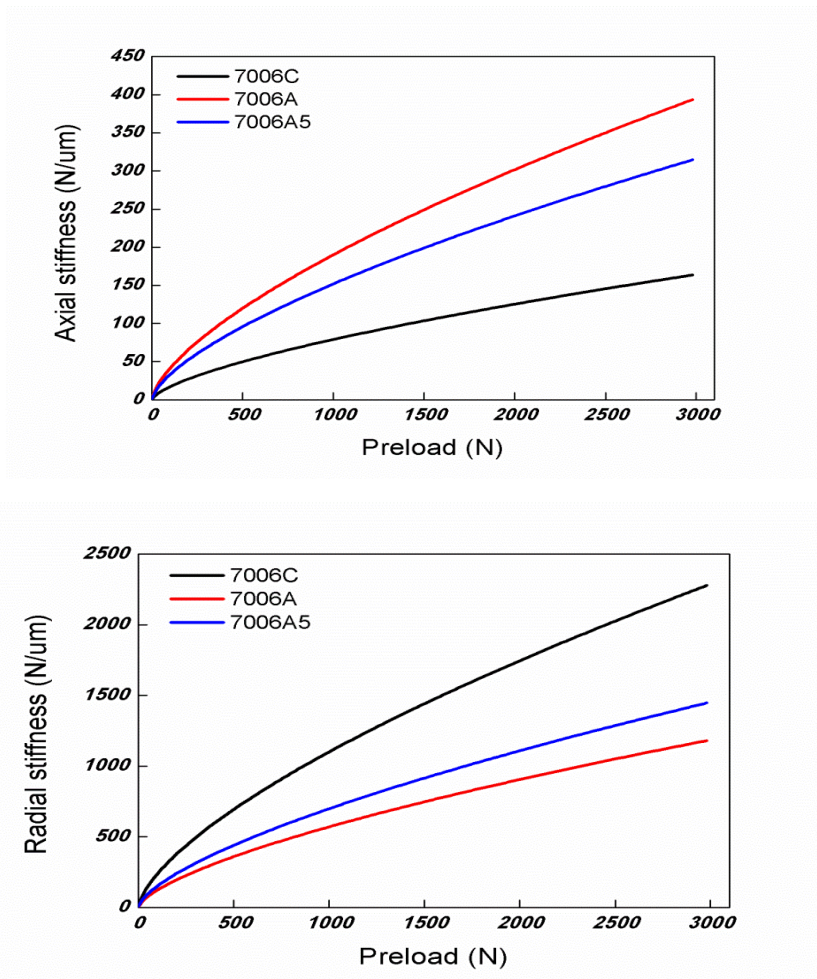


Figure 3.17 Estimation stiffness of bearing stiffness under the preload

IV. FEM prediction of the static/dynamic stiffness of the rotating system

The prediction of static and dynamic stiffness has been conducted by the finite element analysis. The identification process is as follows.

A finite element model of the rotating unit with coupling section was created in first step for angle contact ball bearing. To simulate the stiffness and damping of the coupling section in rotating unit, a spring element has used MATRIX 27 because the angle contact ball bearing had axial and radial stiffness. MATRIX 27 could express stiffness of axial and radial direction in FEM. The arrangement of coupling section consisted of node 16 on inner and outer race. The spindle was made of mild steel, whose elastic modulus $E = 1.90 \times 10^{11}$ Pa, density $\rho = 7850$ Kg/m³ and Poisson's ratio $\mu = 0.3$. The coupling section of the property has been defined in five cases in order to check for a broad spectrum of coupling section.

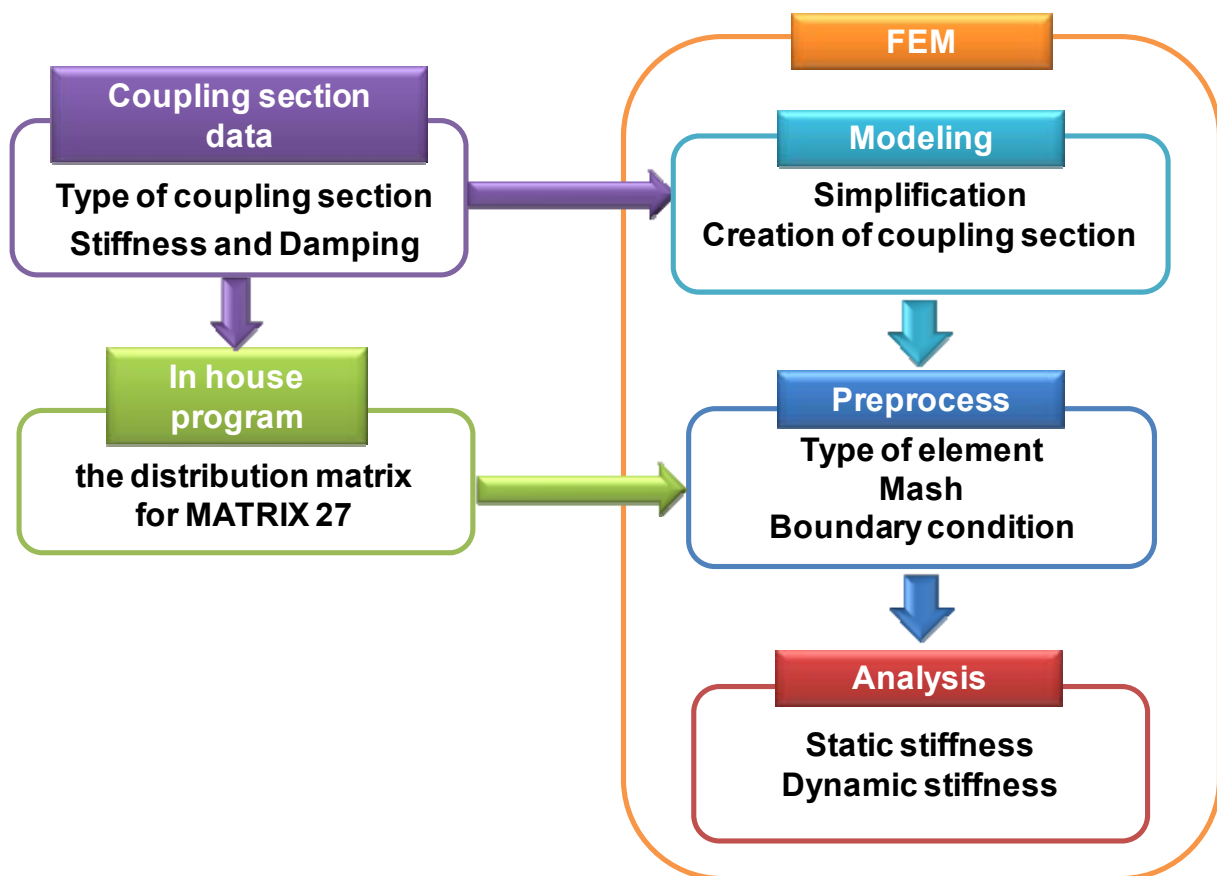


Figure 4.1 Overview of FEM Prediction

In this study, static stiffness is regarded as F/x which is determined by dividing the load F by the end of rotating unit displacement x . For static stiffness, FE model has conducted static analysis. In case of the dynamic stiffness, modal analysis has been carried out. The bearing stiffness had use two cases about estimation data and technical data. Static and dynamic stiffness have difference according to the characteristic of bearings.

Table 2. The technical data of the angular contact ball bearing used in FEM simulation

Manufacturer	Number	Contact angle(°)	Preload (N)	Bearing stiffness (N/ μ m)	
				axial	radial
NSK	7006A	30	50	85	119
	7006A5	25	60	68	136
	7006C	15	39	29	188.5
Nachi	7006C	15	100	21.7	81.1
FAG	7006C	15	75	32.7	196.2

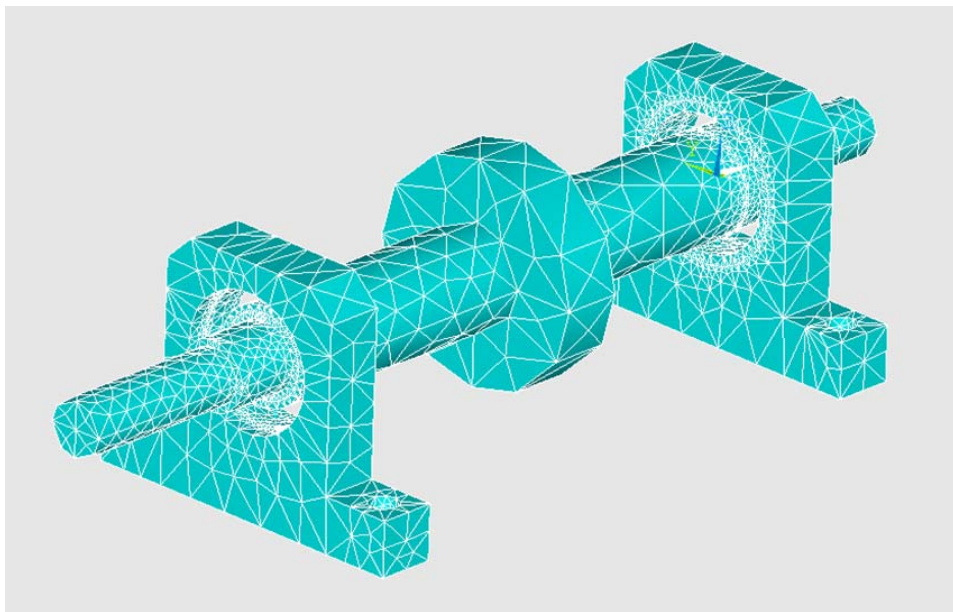
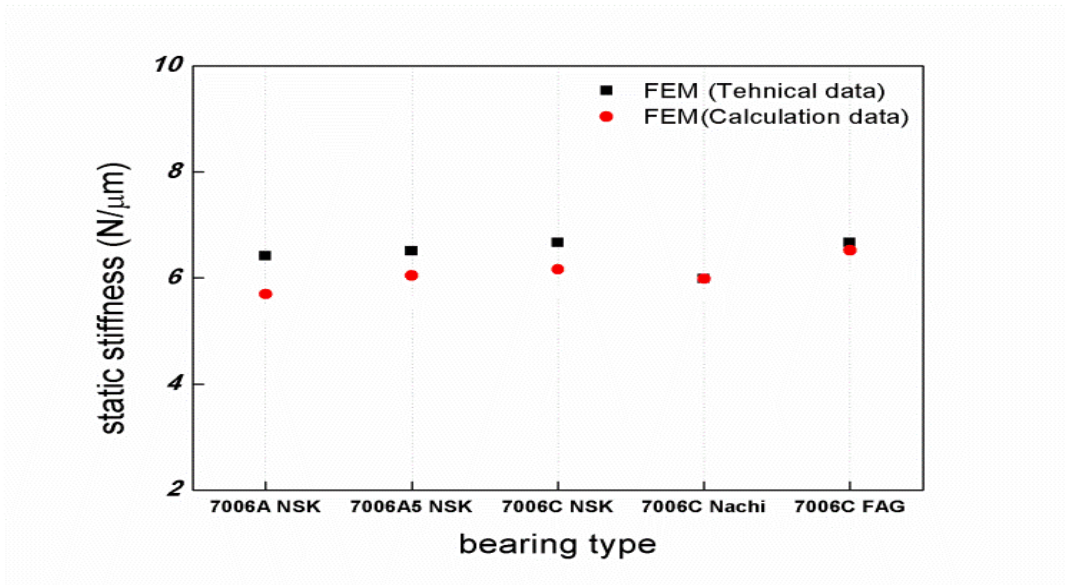
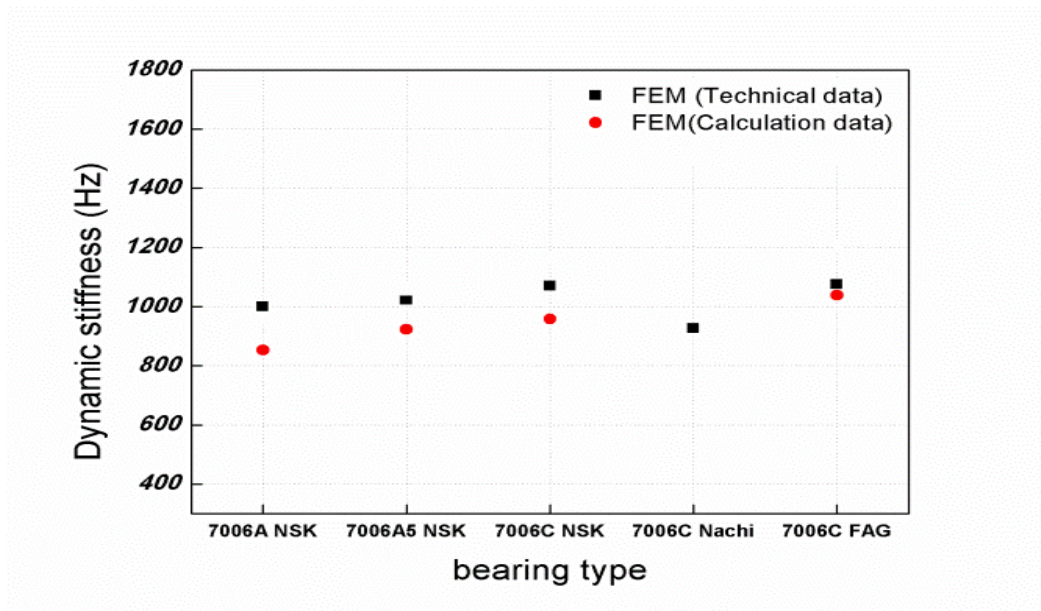


Figure 4.2 The constructed FE model



(a)



(b)

Figure 4.3 Result of static and dynamic stiffness : (a) static stiffness (b) dynamic stiffness

V. Experimental Verification

The prediction model had to need verification for experiment. It has given the evaluation of accuracy for FEM prediction. There was a initial experimental equipment in fig.26. They could do experiments for static and dynamic characteristic. Additionally, the gap sensors and motor are installed in experiment equipment in order to conduct rotor dynamic up on the 3000 RPM. However, It could not considered the preload in experiment equipment. Additional parts have been redesigned for pre-load. To consider the pre-load using bearing nut, The force sensor have been placed at the end of the spindle. It could measure the pre-load for rotating system. Fig. 27 was shown for experiment method.

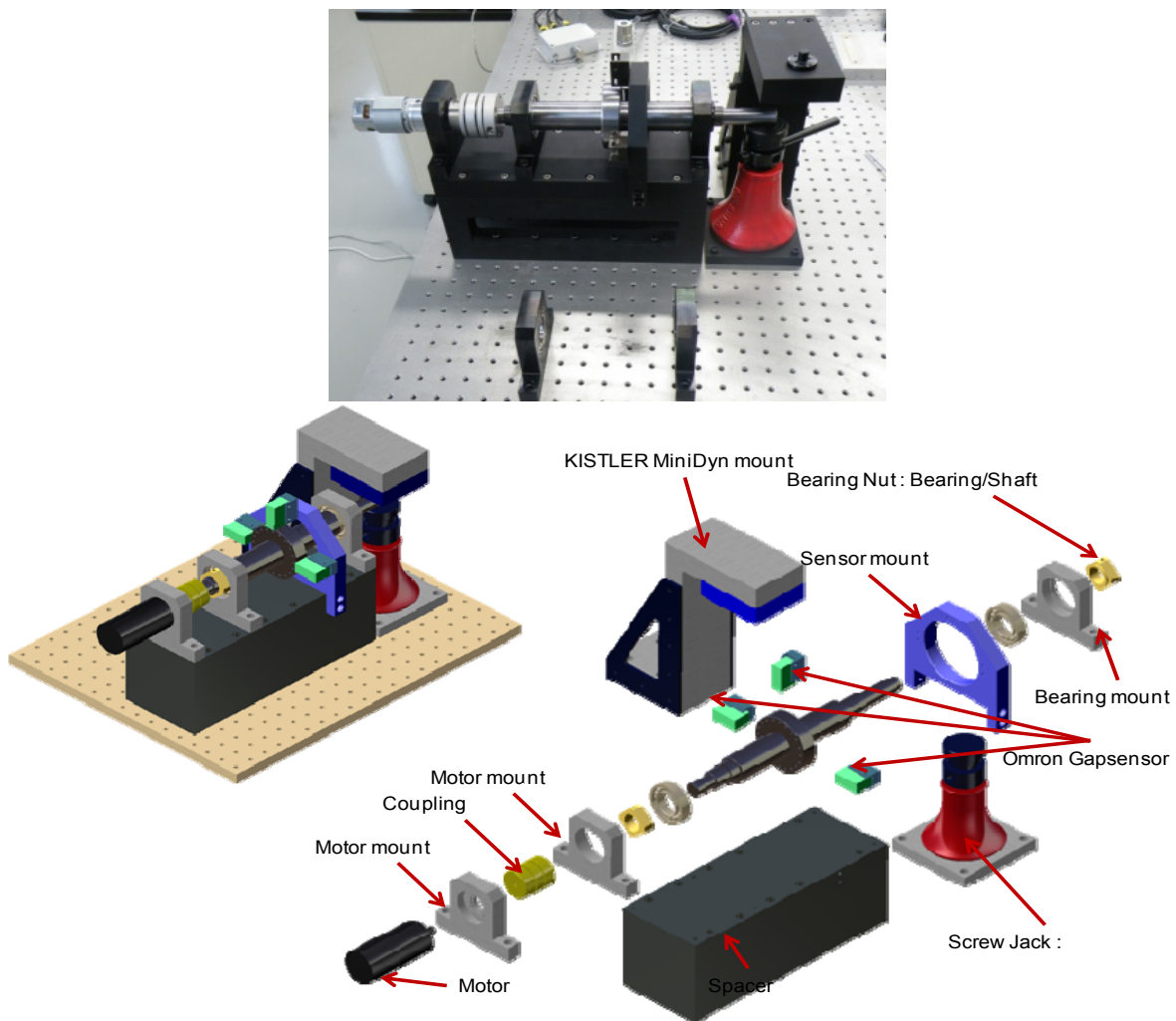


Figure 5.1 Illustration of the experimental setup

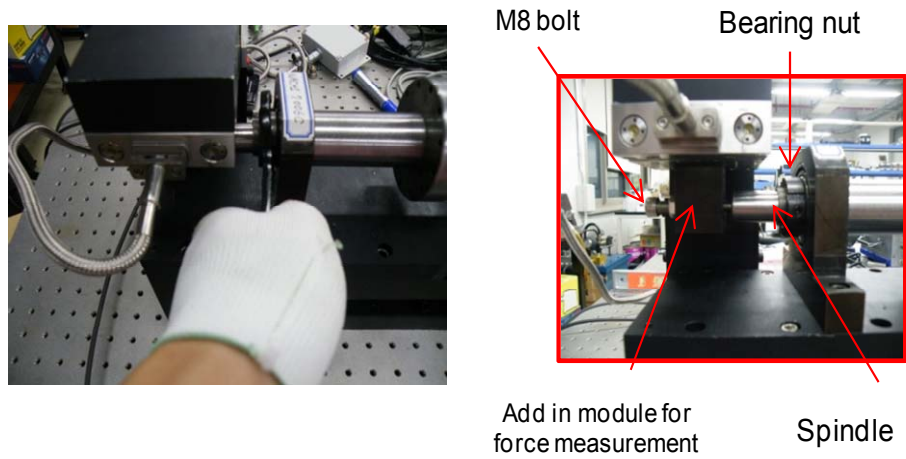


Figure 5.2 Experimental configuration to implement the pre-load

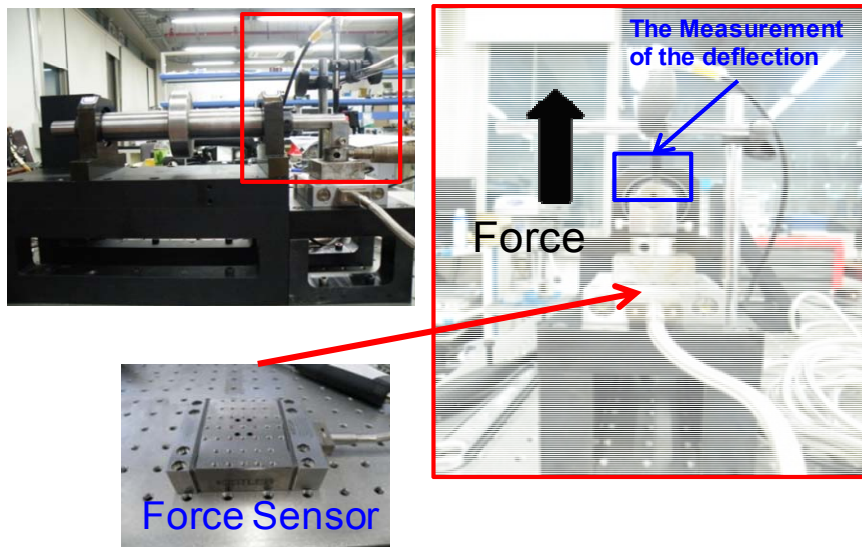


Figure 5.3 Experimental setup to test static stiffness

To compare experiment and FEM result for angular contact ball bearing, five bearing sets have been prepared for experiment. Static stiffness has been conducted at five times each bearing and then a average value was taken. The experimental procedure was that the roll cell generates displacement at the end of the spindle within 0.2mm. In loading condition, a force sensor has collected force value in data acquisition system.

Dynamic stiffness has performed the impact test using the hammer and accelerometer in order to measure the 1st resonance frequency. To avoid the disturbance of structures, the rotating unit have been installed on a rope. The result of FFT have been obtained from data acquisition and then

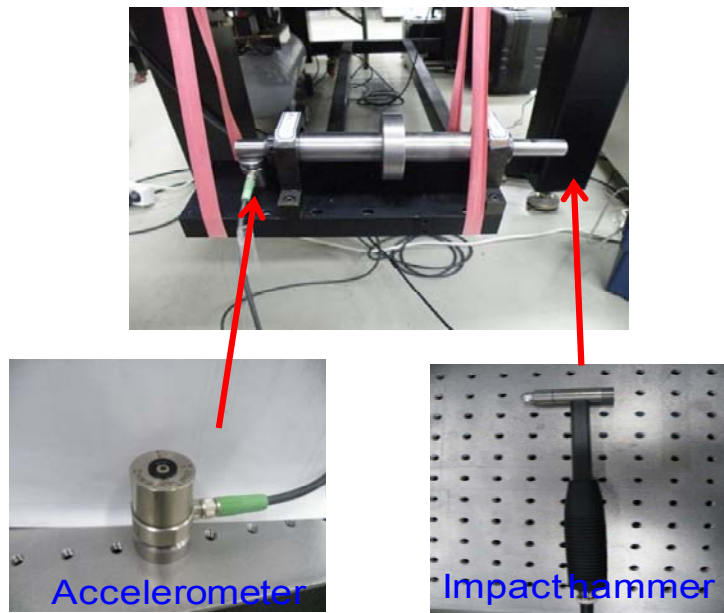


Figure 5.4 Experimental setup to test dynamic stiffness

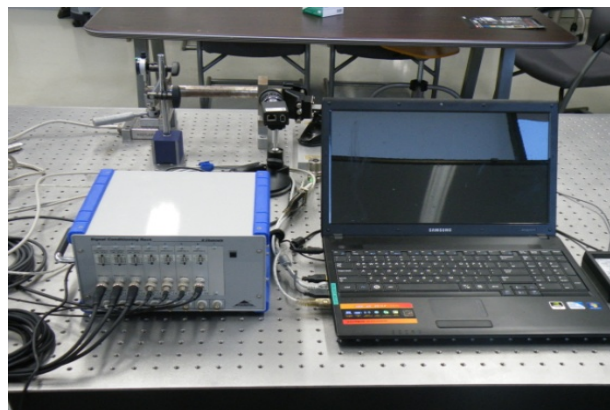
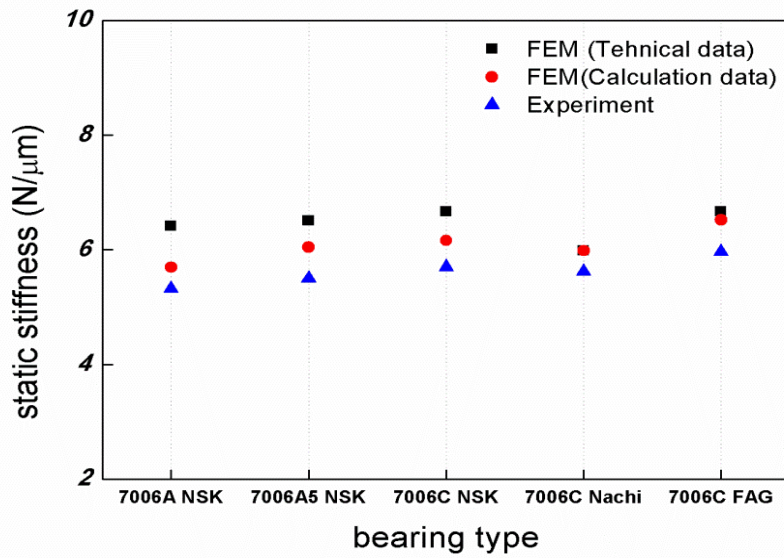
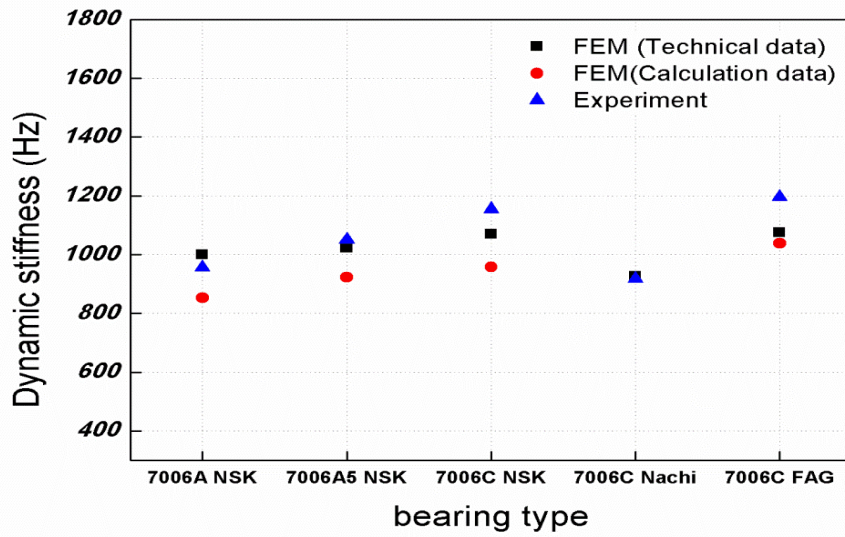


Figure 5.5 Data acquisition system for the experiments

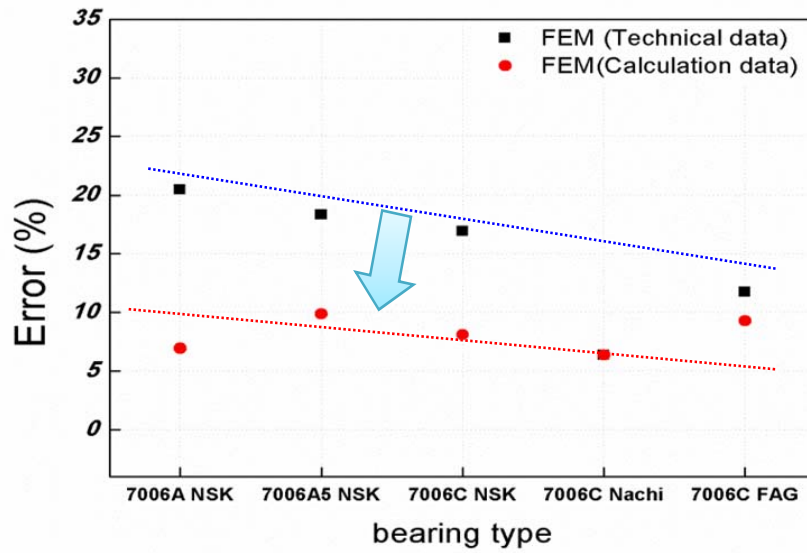


(a)

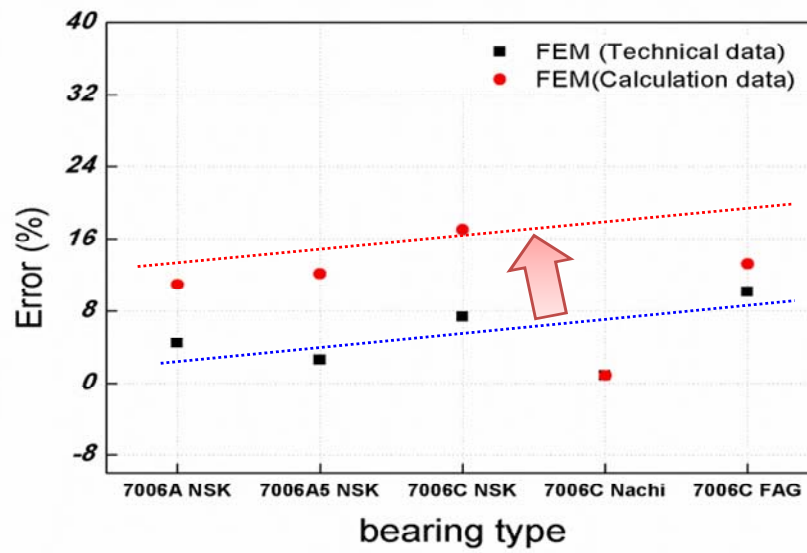


(b)

Figure 5.6 Comparison between FEM prediction and experimental results : (a) static stiffness (b) dynamic stiffness



(a)



(b)

Figure 5.7 The error of FEM predictions : (a) static stiffness (b) dynamic stiffness

The prediction of static and dynamic stiffness in FEM could have followed the trend of experiments. Static stiffness about rotating unit had the average error of 17% within each bearing when the bearing stiffness has obtained the technical data. However, dynamic stiffness has the range of the error within 10% in case of technical data. Although the calculation of bearing stiffness included amount of error, the characteristic of rotating unit could have been expressed. One of advantages was high accuracy in static stiffness.

The Coupling section has high influence about static and dynamic stiffness of rotating system. In particular, Dynamic stiffness has been improved highly. Therefore, FEM model of coupling section couldn't express a momentum stiffness of angular contact ball bearing using MATRIX 27. It could occur the error in FEM. And an experiment case has also limitations. The experiments have been conducted under revolving rotating system. However, it need high technical know-how so it makes experimental error.

VI. FEA automation

Increasing Demands about the 3-D simulation model was through internet. Many of the small companies have need the simulation prediction for their equipments because they have limitations to get the simulation department. If they could predict the characteristic of equipments in design step, they could reduce time and cost to improve the function for the equipment. For making a simulation system based on internet, the simulation method has to develop the generality and automation

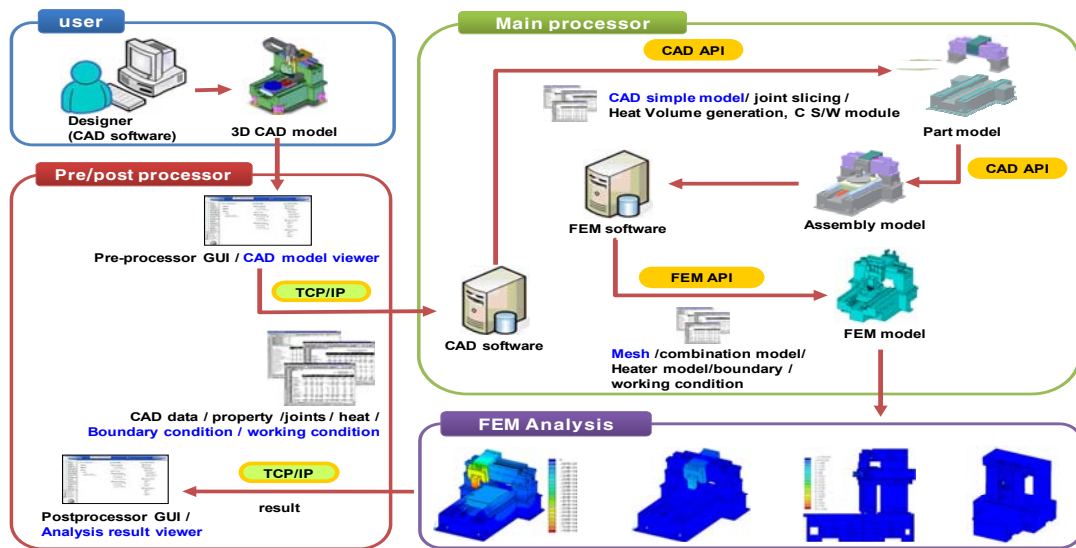


Figure 6.1 Flow simulation based on internet

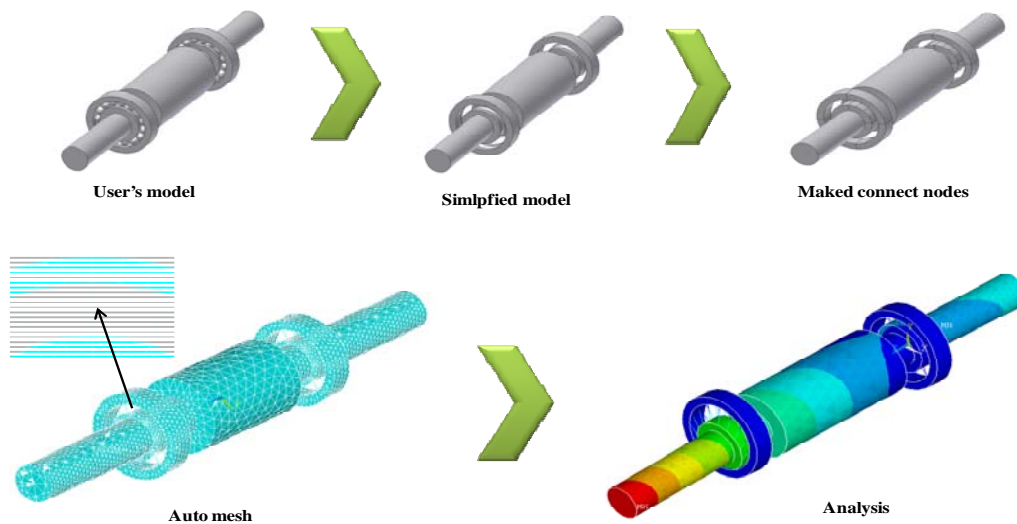


Figure 6.2 Procedure of FEA automation

When bearing stiffness inputted MATRIX 27 in ANSYS, Each spring element has different stiffness matrix depending on local position and global position. If user makes a stiffness matrix for MATRIX 27, many of the procedures have been carried out in each element. Thus, procedures have high sensitivity for making system stiffness for entering data. It has needed to reduce the procedures for user in order to use the element. So this study employed the c language to make automatic calculation for the system matrix. It makes user comfortable during the prediction in ANSYS.

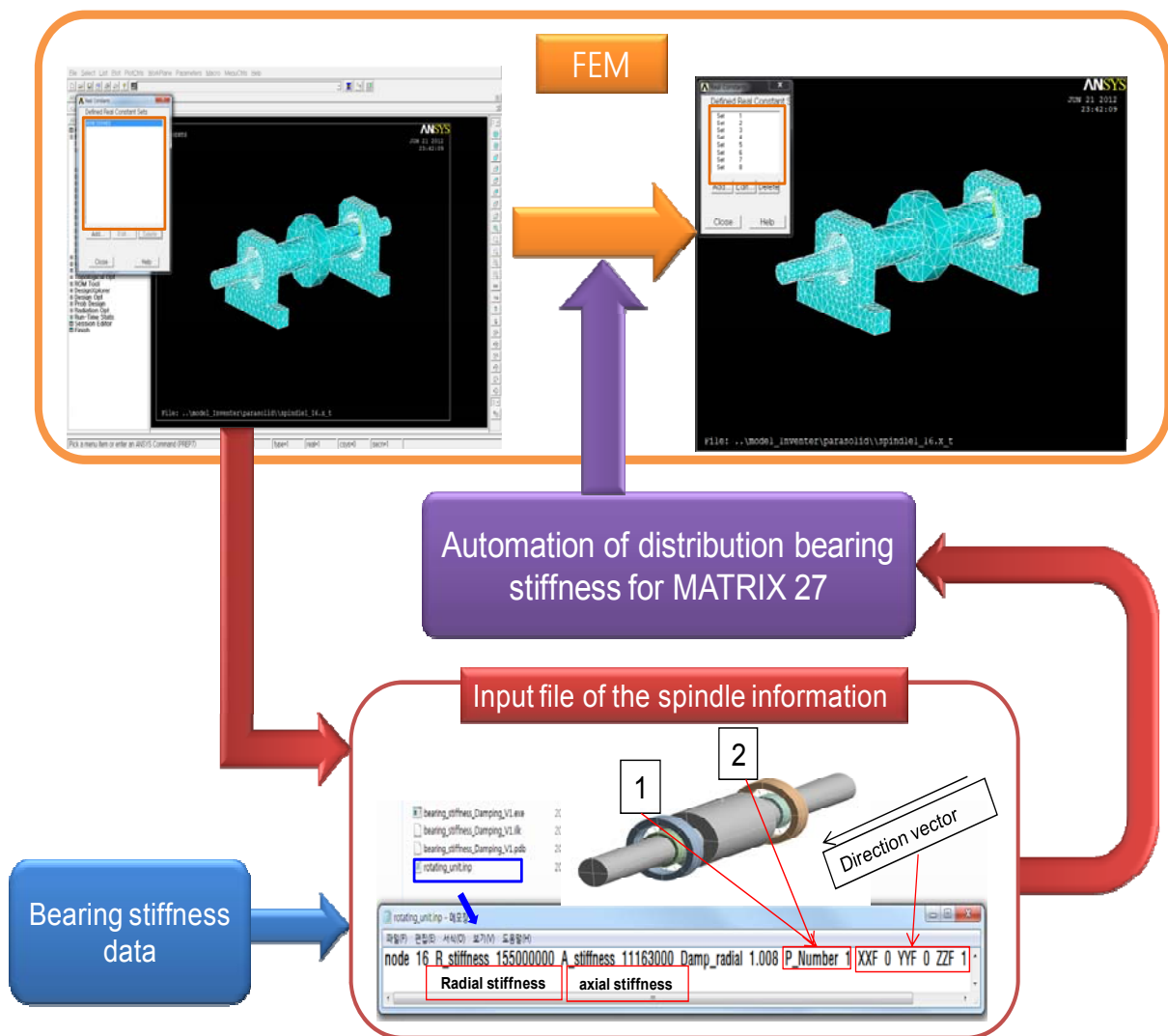


Figure 6.3 Automation of MATRIX 27 for distribution matrix in FEM.

VII. Conclusions

The paper has studied the static and dynamic stiffness of rotating unit with coupling section in FE model. It has been verified by experiments in order to obtain the reliability about FEM.

1. The coupling section of node 16 has made best result about stress distribution, Applied MATRIX 27 and reality.
2. Spring element model have added MATRIX 27 that had the high performances for angular contact ball bearing and model under the specific angle
3. For using MATRIX 27 proficiently, Spring position was important factor to make system matrix
4. Preload effect could not be expressed by preload function of COMBIN 14.
5. Preload has affected the static and dynamic stiffness significantly, so it had to consider the prediction of the procedure.
6. The prediction of characteristic with the angular contact ball bearing has the error of 15% between FEM and experiments. It could predict the trend of static and dynamic stiffness for rotating system in case of considering coupling section.
7. Rotating system has shown high inaccuracy within static stiffness and dynamic stiffness. The reason is that the other terms of coupling section were not considered in the stiffness of spring element such as momentum stiffness. And Experimental approach was also has limitation.

VIII. Future works

During the machining process, there generates a large amount of heat machine tool parts such as electric motor, rolling bearing and cutter. etc.. The heat transfers to different parts of the machine tool by the methods of thermal conduction , convection and radiation, which leads to different temperature rise and thermal expansion for different machine tool parts. Thus, the accurate relative position of the cutter and the work piece is influenced by thermal expansion, which eventually affects the machining accuracy. Errors that affect machining accuracy can be classified as geometric errors, thermal errors and cutting force errors. Amount them, the thermal errors account for 70% of the total errors. Nevertheless, the thermal error of rotating system is very difficult to calculate efficiently, so experience in thermal behavior is key factor in the design process. However, only experience is not enough. Therefore, there is a critical need to develop a systematic modeling tool that can predict the thermal error of rotating system to assist the demand of designer in achieving an optimal design and error compensation.

REFERENCES

1. Kang, Y., et al., Integrated "CAE" strategies for the design of machine tool spindle-bearing systems. *Finite Elements in Analysis and Design*, 2001. 37(6–7): p. 485-511.
2. Rantatalo, M., et al., Milling machine spindle analysis using FEM and non-contact spindle excitation and response measurement. *International Journal of Machine Tools and Manufacture*, 2007. 47(7–8): p. 1034-1045.
3. Mackerle, J., *Finite-element analysis and simulation of machining: a bibliography (1976–1996)*. *Journal of Materials Processing Technology*, 1998. 86(1–3): p. 17-44.
4. Yoonho, S., et al. Structure modeling of machine tools and Internet-based implementation. in *Simulation Conference, 2005 Proceedings of the Winter*. 2005.
5. Cao, Y. and Y. Altintas, Modeling of spindle-bearing and machine tool systems for virtual simulation of milling operations. *International Journal of Machine Tools and Manufacture*, 2007. 47(9): p. 1342-1350.
6. Altintas, Y., et al., Virtual Machine Tool. *CIRP Annals - Manufacturing Technology*, 2005. 54(2): p. 115-138.
7. Zhang, G.P., et al., Predicting dynamic behaviours of a whole machine tool structure based on computer-aided engineering. *International Journal of Machine Tools and Manufacture*, 2003. 43(7): p. 699-706.
8. Mi, L., et al., Effects of preloads on joints on dynamic stiffness of a whole machine tool structure. *Journal of Mechanical Science and Technology*, 2012. 26(2): p. 495-508.
9. Agapiou, J.S., A methodology to measure joint stiffness parameters for toolholder-spindle interfaces. *Journal of Manufacturing Systems*, 2005. 24(1): p. 13-20.
10. Shuzi, Y., A study of the static stiffness of machine tool spindles. *International Journal of Machine Tool Design and Research*, 1981. 21(1): p. 23-40.
11. Agapiou, J.S., ESTIMATING THE STATIC STIFFNESS FOR A SPINDLE-TOOLHOLDER-TOOLING SYSTEM. *Machining Science and Technology*, 2008. 12(1): p. 77-99.
12. Ertürk, A., H.N. Özgüven, and E. Budak, Analytical modeling of spindle-tool dynamics on machine tools using Timoshenko beam model and receptance coupling for the prediction of tool point FRF. *International Journal of Machine Tools and Manufacture*, 2006. 46(15): p. 1901-1912.
13. Bollinger, J.G. and G. Geiger, Analysis of the static and dynamic behavior of lathe spindles. *International Journal of Machine Tool Design and Research*, 1964. 3(4): p. 193-209.
14. Soon, M. and B. Stone, The Optimisation of the Dynamic and Static Stiffness of Spindle Systems, in *International Mechanical Engineering Congress and Exhibition (1994 :Perth, W.A.)1994*, Institution of Engineers, Australia: Barton, A.C.T. p. 233-238.
15. Wardle, F.P., S.J. Lacey, and S.Y. Poon, Dynamic and static characteristics of a wide speed range machine tool spindle. *Precision Engineering*, 1983. 5(4): p. 175-183.
16. Kim, K.J., K.F. Eman, and S.M. Wu, Identification of natural frequencies and damping ratios of machine tool structures by the dynamic data system approach. *International Journal of Machine Tool Design and Research*, 1984. 24(3): p. 161-169.
17. Zapciu, M.C., Olivier; Bisu, Claudiu-Florinel; Gérard, Alain; K'Nevez, Jean-Yves, Experimental study of machining system: dynamic characterization. *J. of Machin. and Form*, 08/2009. *Technol. 1, 3-4 (2009) (J. of Machin. and Form. Technol. 1, 3-4 (2009) 1-18)*: p. 1-18.
18. Wensing, J.A. and G.C. van Nijen, The dynamic behaviour of a system that includes a rolling bearing. *Proceedings of the Institution of Mechanical Engineers, Part J: Journal of Engineering Tribology*, 2001. 215(6): p. 509-518.
19. Schulz, H. and T. Moriwaki, High-speed Machining. *CIRP Annals - Manufacturing Technology*, 1992. 41(2): p. 637-643.
20. Yamazaki, T., et al., Measurement of Spindle Rigidity by using a Magnet Loader. *Journal of*

- Advanced Mechanical Design, Systems, and Manufacturing*, 2010. 4(5): p. 985-994.
21. Albrecht, A., et al., High frequency bandwidth cutting force measurement in milling using capacitance displacement sensors. *International Journal of Machine Tools and Manufacture*, 2005. 45(9): p. 993-1008.
 22. Shamine, D.M., S.W. Hong, and Y.C. Shin, Experimental Identification of Dynamic Parameters of Rolling Element Bearings in Machine Tools. *Journal of Dynamic Systems, Measurement, and Control*, 2000. 122(1): p. 95-101.
 23. Gagnol, V., T.-P. Le, and P. Ray, Modal identification of spindle-tool unit in high-speed machining. *Mechanical Systems and Signal Processing*, 2011. 25(7): p. 2388-2398.
 24. Gagnol, V., et al., Model-based chatter stability prediction for high-speed spindles. *International Journal of Machine Tools and Manufacture*, 2007. 47(7-8): p. 1176-1186.
 25. Mañé, I., et al., Stability-based spindle speed control during flexible workpiece high-speed milling. *International Journal of Machine Tools and Manufacture*, 2008. 48(2): p. 184-194.
 26. Zverv, I., et al., An elastic deformation model of high speed spindles built into ball bearings. *Journal of Materials Processing Technology*, 2005. 170(3): p. 570-578.
 27. Deping Liu, H.Z., Zheng Tao and Yufeng Su, Finite element analysis of High speed motorized spindle based on ANSYS. *The open Mechanical Engineering Journal*, 2011. 5(5): p. 1-10.
 28. Kolar, P., M. Sulitka, and M. Janota, Simulation of dynamic properties of a spindle and tool system coupled with a machine tool frame. *The International Journal of Advanced Manufacturing Technology*, 2011. 54(1): p. 11-20.
 29. Wu, Y.-D., L. Jian-Fa, and B.-L. Li. Finite element analysis and experimental study on spindle of boring-milling machine. in *Computer Design and Applications (ICDDA), 2010 International Conference on*. 2010.
 30. Hung, J., Load effect on the vibration characteristics of a stage with rolling guides. *Journal of Mechanical Science and Technology*, 2009. 23(1): p. 89-99.
 31. Yuan Lin, C., J. Pin Hung, and T. Liang Lo, Effect of preload of linear guides on dynamic characteristics of a vertical column-spindle system. *International Journal of Machine Tools and Manufacture*, 2010. 50(8): p. 741-746.
 32. Weiguang, L., et al. ANSYS-Based Dynamic Analysis of High-Speed Motorized Spindle. in *Computer Engineering and Technology, 2009. ICCET '09. International Conference on*. 2009.
 33. Meng, L. and G. Qunying. Dynamic analysis and optimization of small size motorized spindle-toolholder system. in *Computer, Mechatronics, Control and Electronic Engineering (CMCE), 2010 International Conference on*. 2010.
 34. Gagnol, V., et al., Dynamic Analyses and Design Optimization of High-Speed Spindle-Bearing System
Advances in Integrated Design and Manufacturing in Mechanical Engineering II, S. Tichkiewitch, M. Tollenaere, and P. Ray, Editors. 2007, Springer Netherlands. p. 505-518.
 35. Abele, E., Y. Altintas, and C. Brecher, Machine tool spindle units. *CIRP Annals - Manufacturing Technology*, 2010. 59(2): p. 781-802.
 36. Hwang, Y.K. and C.M. Lee, Development of automatic variable preload device for spindle bearing by using centrifugal force. *International Journal of Machine Tools and Manufacture*, 2009. 49(10): p. 781-787.
 37. Hwang, Y.-K. and C.-M. Lee, A review on the preload technology of the rolling bearing for the spindle of machine tools. *International Journal of Precision Engineering and Manufacturing*, 2010. 11(3): p. 491-498.
 38. Cao, H., T. Holkup, and Y. Altintas, A comparative study on the dynamics of high speed spindles with respect to different preload mechanisms. *The International Journal of Advanced Manufacturing Technology*, 2011. 57(9): p. 871-883.
 39. D. Herákl, R.C., A. Sedláček, E. Janča, Exploitation of Hertz's contact pressures in friction drives. *RES. AGR. ENG*, 2006 52(3): p. 107-114.

Acknowledgement

I would like to express my sincere gratitude and thanks to Professor Hynug Wook Park for his extensive support throughout the program and guidance as a thesis advisor. I also would like to thank my committee members, Professors Young-Bin Park and Duck-Young Kim for their suggestion and assistance during the preparation of this thesis. A sincere appreciation goes to all my co-workers of Mechanical and Advanced Materials Engineering particularly my lab-maters, Jae woo and Dong-min, for their help and meaningful contribution to the thesis. Finally, I would like to thank my parents and friends for their encouragement and support throughout my life and education.

APPENDIX

MATRIX 27 software code.

```
#include<stdio.h>
#include<stdlib.h>
#include<direct.h>
#include<stdio.h>
#include<math.h>
#include<string.h>
#include<stdlib.h>
#include<sys/types.h>

double TMC(int a, int b,double c[3][3],double d[3][3],double e[3][3])
{
    int i,j;
    double T[3][3],result;
    for(i=0;i<=2;i++)
    {
        for(j=0;j<=2;j++)
        {
            T[i][j] = (c[i][0]*d[0][j])+(c[i][1]*d[1][j])+(c[i][2]*d[2][j]);
        }
    }
    result= (T[a][0]*e[0][b])+(T[a][1]*e[1][b])+(T[a][2]*e[2][b]);
    return result;
}

char * filename (char *str1, char *str2,char *str3,char *str4)
{
    int len1, len2,len3,len4;
```

```

char *newstr,*ptr;
len1 = strlen(str1);
len2 = strlen(str2);
len3 = strlen(str3);
len4 = strlen(str4);
newstr = (char *)malloc(len1+len2+len3+len4+1);
ptr = (char *)memcpy(newstr,str1,len1);
ptr = (char *)memcpy(ptr+len1,str2,len2);
ptr = (char *)memcpy(ptr+len2,str3,len3);
ptr = (char *)memcpy(ptr+len3,str4,len4);
ptr = ptr + len4;
*ptr= '\0';
return(newstr);
}

int main(int argc,char **argv)
{
int i,j,k,p,q,s;
double pi=3.1415926535897932384626433832795;
float K_axis,K_radial,D_radial,f_x1,f_y1,f_z1;
int state,state1,node=0;
double K_D_radial,K_D_axis,D_D_radial;
double a1,a2,a3,a4,b1,b2,b3,b4,ap,beta,gama,sets;
double KMX[3][3],DMX[3][3],M_RTM[3][3],M_RTM_T[3][3]
double M_DDM[3][3],M_DDM_T[3][3],K_ISM[3][3],K_DSM[3][3],K_DSM1[3][3];
double a,b,c,L,L1,de;
char nc[128],krc[128],kac[128],dam[128],x1c[128],y1c[128],z1c[128],PN[128],PN1[3];
char *pilter="bearing_stiffness_damping_V1.exe";
char *ST_Name="bearing_stiffness_ ", *ST_Name1=".sff";
char *IN_Name="rotating_ ",*IN_Name1="unit",*IN_Name2=".inp";
char *inp_Name, *sff_Name;
char *pathname,pathname1[_MAX_PATH],pathname2[_MAX_PATH];
pathname=argv[0];

```



```

i=0;
while(*(pathname+0)!=NULL)
{
    pathname1[i]=*(pathname+i);
    if (*(pathname + i)== NULL)
    {
        pathname1[i] ='\0';
        break ;
    }
    i=i+1;
}
i=0;
j=0;

while (pathname1[0] != NULL)
{
    if (pathname1[i]==pathname1[2])
    {
        pathname2[j]= pathname1[2];
        j=j+1;
        pathname2[j]= pathname1[2];
    }

    else if ( pathname1[i]==NULL)

    {
        j=j-strlen(pilter);
        pathname2[j]='\0';
        break;
    }
    else
    {
        pathname2[j]=pathname1[i];

```

```

        }
        i=i+1;
        j=j+1;
    }
    inp_Name=filename(pathname2,IN_Name,IN_Name1,IN_Name2);
    FILE * file= fopen(inp_Name,"rt");
    if(file==NULL){
        printf("file open error !\n");
        return 1;
    }
    fscanf(file,"%s %d %s %f %s %f %s %f %s %s %s %f %s %f %s %f",&nc,&node,&krc,&K_r
        adial,&kac,&K_axis,&dam,&D_radial,&PN,&PN1,&x1c,&f_x1,&y1c,&f_y1,&z1c,&f_z1);
    state=fclose(file);
    if(state!=0){
        printf("file close error!\n");
        return 1;
    }
    sff_Name=filename(pathname2,ST_Name,PN1,ST_Name1);
    FILE * file1 = fopen(sff_Name,"w");
    if(file1==NULL){
        printf("file1 open error!\n");
        return 1;
    }
    if(abs(f_x1)<0.001)
    {
        f_x1=0;
    }
    if(abs(f_y1)<0.001)
    {
        f_y1=0;
    }
    if(abs(f_z1)<0.001)
    {

```

```

        f_z1=0;
    }

    K_D_radial=K_radial/(node*0.25);
    K_D_axis=K_axis/(node*0.5);
    D_D_radial=D_radial/(node*0.25);

    for(i=0;i<=2;i++)
    {
        for(j=0;j<=2;j++)
        {
            KMX[i][j]=0;
            DMX[i][j]=0;
            de=0;
        }
    }
    KMX[0][0]=K_D_radial;
    KMX[2][2]=K_D_axis;
    DMX[0][0]=D_D_radial;

    a=(f_x1)*(f_x1);
    b=(f_y1)*(f_y1);
    c=(f_z1)*(f_z1);

    L=sqrt(b+c);
    ap=asin((f_y1)/L);
    L1=sqrt(a+c);
    beta=acos((f_z1)/L1);

    if(b==0 && c==0)
    {
        ap=0;
    }

```

```

if(a==0 && c==0)
{
    beta=0;
}
gama=0;
a2=cos(ap);b2=sin(ap);
a3=cos(beta);b3=sin(beta);
a4=cos(gama);b4=sin(gama);
double Rx[3][3]={ {1,0,0}, {0,a2,-b2}, {0,b2,a2} };
double Ry[3][3]={ {a3,0,b3}, {0,1,0}, {-b3,0,a3} };
double Rz[3][3]={ {a4,b4,0}, {-b4,a4,0}, {0,0,1} };
for(i=0;i<=2;i++)
{
    for(j=0;j<=2;j++)
    {
        M_RTM[i][j]=TMC(i,j,Rx,Ry,Rz);
    }
}
for(p=0;p<=2;p++)
{
    for(q=0;q<=2;q++)
    {
        M_RTM_T[q][p]=M_RTM[p][q];
    }
}

seta=0;
for(s=0;s<=(node*0.5)-1;s++)
{

    a1=cos(seta);b1=sin(seta);
    double M_DSM[3][3]={ {a1,b1,0}, {-b1,a1,0}, {0,0,1} };
    de=de+(360.0/(node));
}

```

```

seta=(pi/180)*de;
for(i=0;i<=2;i++)
{
    for(j=0;j<=2;j++)
    {
        M_DDM[i][j]=TMC(i,j,M_RTM,M_DSM,M_RTM_T);
    }
}

for(j=0;j<=2;j++)
{
    for(k=0;k<=2;k++)
    {
        M_DDM_T[k][j]=M_DDM[j][k];
    }
}

if(s%2==0)
{
    for(i=0;i<=2;i++)
    {
        for(j=0;j<=2;j++)
        {
            K_ISM[i][j]=TMC(i,j,M_RTM,KMX,M_RTM_T);
        }
    }
    for(i=0;i<=2;i++)
    {
        for(j=0;j<=2;j++)
        {
            K_DSM[i][j]=TMC(i,j,M_DDM,K_ISM,M_DDM_T);
            K_DSM1[i][j]=-K_DSM[i][j];
            if (abs(K_DSM[i][j]) <=0.00000001)
            {

```

```

        K_DSM[i][j]=0;
    }

    if (abs(K_DSM1[i][j]) <=0.00000001)
    {
        K_DSM1[i][j]=0;
    }
}

}
else
{
    for(i=0;i<=2;i++)
    {
        for(j=0;j<=2;j++)
        {
            K_ISM[i][j]=TMC(i,j,M_RTM,DMX,M_RTM_T);
        }
    }
    for(i=0;i<=2;i++)
    {
        for(j=0;j<=2;j++)
        {
            K_DSM[i][j]=TMC(i,j,M_DDM,K_ISM,M_DDM_T);
            K_DSM1[i][j]=-K_DSM[i][j];
            if (abs(K_DSM[i][j]) <=0.00000001)
            {
                K_DSM[i][j]=0;
            }

            if (abs(K_DSM1[i][j]) <=0.00000001)
            {

```

```

                                K_DSM1[i][j]=0;
                                }
                            }
                    }
            }

printf("%f,%f,%f,%f,%f,%f,%f,%f,%f,%f\n",de22.5,K_DSM[0][0],K_DSM[0][1],K_DSM[0][2],K_DS
M[1][0],K_DSM[1][1],K_DSM[1][2],K_DSM[2][0],K_DSM[2][1],K_DSM[2][2]);

fprintf (file1,"R,%d,%f,%f,%f,,,\n",s+1,K_DSM[0][0],K_DSM[0][1],K_DSM[0][2]);
        fprintf(file1,"RMORE,%f,%f,%f,,,\n",K_DSM1[0][0],K_DSM1[0][1],K_DSM1[0][2]);
        fprintf (file1,"RMORE,%f,%f,,,\n",K_DSM[1][1],K_DSM[1][2],K_DSM1[1][0]);
        fprintf (file1,"RMORE,%f,%f,,,\n",K_DSM1[1][1],K_DSM1[1][2],K_DSM[2][2]);
        fprintf(file1,"RMORE,,,\n",K_DSM1[2][0],K_DSM1[2][1],K_DSM1[2][2]);
        fprintf (file1,"RMORE,,,,,\n");
        fprintf (file1,"RMORE,,,,,\n");
        fprintf (file1,"RMORE,,,,,\n");
        fprintf (file1,"RMORE,,,,,\n");
        fprintf (file1,"RMORE,,,\n",K_DSM[0][0],K_DSM[0][1],K_DSM[0][2]);
        fprintf (file1,"RMORE,,,\n",K_DSM[1][1],K_DSM[1][2]);
        fprintf (file1,"RMORE,,,\n",K_DSM[2][2]);
        fprintf (file1,"RMORE,,,,,\n\n");
    }
    state1=fclose(file1);
    if(state1!=0)
    {
        printf("file close error !\n");
        return 1;
    }
    return 0;
}

```

Bearing stiffness calculation code.

```
Dim ba As Double, gs As Double, pl As Double
Dim nb As Double, ca As Double
Dim m As Double, Er As Double
Dim pi As Double, beta As Double
Dim p_ball As Double, F1 As Double, F2 As Double
Dim P_h As Double, de As Double, de_t As Double, de_r As Double, de_a As Double
Dim K_a As Double, K_r As Double, Cal_a As Double, Cal_r As Double
ba = ball_size.Value
gs = 1.15 * ba
pl = preload.Value
nb = number_balls.Value
ca = contact_angle.Value

Er = 226000000000#
m = 0.45
pi = 3.14159265358979
beta = (pi / 180) * ca
F1 = pl
p_ball = F1 / (nb * Sin(beta))
F2 = nb * p_ball * Cos(beta)
P_h = (4 * (1 - ba / gs)) / ba
de = (3 * p_ball) / (Er * P_h)
de_t = 2 * m * ((de) ^ (1 / 3))
de_a = de_t / Sin(beta)
de_r = de_t / Cos(beta)
If F1 < 120 Then
Cal_a = 2.87
Cal_r = 1.31415463
```



```
ElseIf F1 >= 120 And F1 <= 300 Then
```

```
    Cal_a = 2.070564039
```

```
    Cal_r = 0.888743716
```

```
ElseIf F1 > 300 And F1 <= 500 Then
```

```
    Cal_a = 1.850756407
```

```
    Cal_r = 0.693092568
```

```
ElseIf F1 > 500 And F1 <= 1000 Then
```

```
    Cal_a = 1.550756407
```

```
    Cal_r = 0.703092568
```

```
Else
```

```
    Cal_a = 1.680731758
```

```
    Cal_r = 0.78738479
```

```
End If
```

```
K_a = (F1 / de_a) * 0.001 * Cal_a
```

```
K_r = (F2 / de_r) * 0.001 * Cal_r
```

```
Range("a").Cells = K_a
```

```
Range("b").Cells = K_r
```

```
Range("sum").Cells = de_t
```

```
End Sub
```